GEOLOGICAL JOURNAL
Geol. J. (2014)
Published online in Wiley Online Library
(wileyonlinelibrary.com). DOI: 10.1002/gj.2623

The upper Viséan–Serpukhovian in the type area for the Serpukhovian Stage (Moscow Basin, Russia): Part 2. bulk geochemistry and magnetic susceptibility

PAVEL B. KABANOV[1,2]*, ANDREY O. ALEKSEEV[3] and TIKHON ZAITSEV[4]

[1] *Geological Survey of Canada (Calgary), Calgary, AB, Canada*
[2] *Kazan Federal University, Kazan, Russia*
[3] *Institute of Physical, Chemical, and Biological Problems of Soil Science (ISSP) RAS, Pushchino, Russia*
[4] *Geological Faculty, M.V. Lomonosov Moscow State University, Moscow, Russia*

This study is the summary analysis of bulk XRF geochemistry (233 samples from three sections) of the Oka and Zaborie groups of the type Serpukhovian succession in the Moscow Basin. The siliciclastic wedges in the limestone-dominated Oka Group are two to three times enriched in Fe, Ti, and Zr compared to Clarke values. Bulk iron strongly correlates with magnetic susceptibility. Iron tends to form ferruginized horizons (original siderites) in finer grained siliciclastic beds associated with coal seams. These beds also tend to be enriched in Cu, Ni, Pb, Zn, and other trace metals (metal enrichment horizons or MEHs). MEHs formed in ponded conditions of coastal low-pH marshlands vegetated by mangrove-like lycopsid bushes. Well-drained environments of palaeokarst formation and alkaline everglades (Akulshino palustrine event) on the other hand did not accumulate Fe and trace metals. The thin shale seam (found close to the Viséan–Serpukhovian boundary in Polotnyanyi Zavod) has unusually high Rb and Sr values, which may contain volcanigenic material useful for absolute dating. The Gurovo Formation (Steshevian Substage of the Serpukhovian) is less enriched in Fe and Ti. In the Gurovo Formation, the transition from the lower montmorillonitic shale (Glazechnya Member) to the upper palygorskitic shale (Dashkovka Member) is expressed by a five-fold increase in background MgO values, which indicates progressive shoaling and climatic aridization. Phosphorus remains close to 0% in the Oka Group and tends to increase in the Zaborie Group, in agreement with a dramatic increase of conodont numbers and other signatures of a lower Serpukhovian marine transgression. The lower half of the Glazechnya Member exhibits fluctuating enrichment in Fe, Cu, Ni, Pb, Zn, V, Cr, and Co. These fluctuations are mostly inverse to fluctuations of Mn. This pattern has been interpreted as a signature of seafloor oxygen deficiency, where Mn-rich samples record oxygen-poor environments (redox barrier level with the sediment surface) and Mn-poor samples enriched in Fe and trace metals record transitions to anoxic setting. This interval is interpreted as the Lower Serpukhovian highstand. Enrichment in Fe, Ti, and Zr of Oka siliciclastic units of Polotnyanyi Zavod indicates provenance from the ore-rich Voronezh Land, south of the Moscow Basin. The westerly flux regarded as a possible provenance in previous palaeogeographic reconstructions is discarded for the studied sections. The Gurovo Shale is also linked to the Voronezh province, although Fe, Ti, and Zr concentrations are lower than in the Oka shales. Copyright © 2014 John Wiley & Sons, Ltd.

Received 25 April 2014; accepted 25 September 2014

KEY WORDS XRF geochemistry; Mississippian; Moscow basin; provenance; fluvial wedges; shale basin; trace metals; magnetic susceptibility

1. INTRODUCTION

This companion paper adds XRF geochemical information to a multifaceted stratigraphic description of the type succession of the Serpukhovian Stage and the underlying Oka Group (Kabanov *et al*., 2014). These bulk geochemical data are supplemented by lab measurements of magnetic susceptibility (MS) undertaken on the same samples. Parts of this XRF-MS dataset have been reported in preceding project papers (Alekseev *et al*., in press; Kabanov *et al*., 2012), but the data from the Oka Group of the Novogurovsky section are published here for the first time. The total dataset collected during the period 2006–2013 is the first publicly available geochemical survey of the studied succession. In previous decades, 'semiquantitative' geochemical characterization on minor and rare elements had been given by Makhlina *et al*. (1993) based on two wells from the southern flank of the Voronezh High (northern monocline of the Dnieper–Donets Basin). These characteristics, averaged per regional substage, were extrapolated to the Moscow Basin (Makhlina *et al*., 1993). Some interesting findings of Makhlina *et al*. (1993) were the prominent enrichment of Ti, Cr, and Co in the Tulian,

*Correspondence to: P. B. Kabanov, Geological Survey of Canada (Calgary), Alberta, Canada. E-mail: Pavel.Kabanov@rncan-nrcan.gc.ca

Aleksinian, and Mikhailovian substages, and also the significantly elevated content of vanadium in the Tulian.

In this paper we summarize bulk geochemical information from three quarry sections aiming to tackle previously unknown details of the studied sedimentary system in terms of authigenic *vs.* detrital siliciclastic geochemical signatures, the redox history of the sediments, and the imprint of base-level fluctuations.

2. STRATIGRAPHY, FACIES AND DIAGENETIC HISTORY

The studied sedimentary succession is a thin, stratigraphically complex, carbonate-dominated package (Fig. 1) described in detail by Kabanov *et al*. (2014). Its upper Viséan–basal Serpukhovian part contains numerous disconformities and several siliciclastic wedges developed from either the W or SW and thinning out to the E and NE over a lateral distance of tens of kilometres (Fig. 1; Birina *et al*., 1971; Makhlina *et al*., 1993; Kabanov *et al*., 2014). The lower Serpukhovian Zaborie Group (Tarusa and Gurovo formations) records a transgression and progradation of a relatively large although low-energy delta that supplied fine siliciclastics to the delta-front shale basin (Kabanov *et al*., 2012, 2014). It should be noted that here and in the companion Part 1 paper (Kabanov *et al*., 2014), conventional use of regional substages (Aleksinian, Mikhailovian, Venevian, Tarusian, Steshevian, and Protvian) is abandoned in favour of formations (Aleksin (oldest), Mikhailov, Venev, Tarusa, Gurovo, and Protva; Fig. 1), which is dictated by the need for more consistent use of lithostratigraphic nomenclature (Kabanov *et al*., 2014). The Gurovo Formation is a new name for the Steshevian Substage in the type Serpukhovian succession introduced by Kabanov *et al*. (2014). The lateral extent of the Gurovo Formation approximates the limits of the facies zone I in Figure 2B where it is predominantly composed of dark-coloured shales, in contrast to the type Steshevian (Steshevo Formation) *ca*. 250 km to the NW of the studied area, where the Steshevian is composed of limestones and dolostones interbedded with relatively thin shales (Birina *et al*., 1971; Makhlina *et al*., 1993). The Gurovo Formation is composed of three members: the lower Glazechnya Member (dark grey to black montmorillonitic shales with limestone lenses and shale-limestone alternation in the basal 1–3 m), a middle Dashkovka Member (steel grey palygorskitic shales with dolostone and limestone intercalations), and an upper Kremenskoe Member, dominated by cherty ostracodal limestones with oncoids (Fig. 1; Kabanov *et al*., 2014). The sequences and parasequences of the studied succession are defined by disconformities and shoaling levels (Kabanov *et al*., 2013, 2014). For the sake of simplicity, unless sequence boundaries appear to coincide with boundaries of previously established formations and members (Fig. 1), the sequence stratigraphic units are not further discussed in this paper.

Deposition in an epeiric-sea setting in the central part of the East European Craton (EEC) (Fig. 2; Nikishin *et al*., 1996) rendered some non-actualistic facies features discussed in Part 1 of this study (Kabanov *et al*., 2014). Bulk geochemical signals show a similar complexity (Alekseev *et al*., in press). The succession never experienced deep burial and preserves many primary features such as clay mineral associations and magnetic signals of the rock matrix. On the other hand, protracted exposures in near-surface aquifers and karst processes have caused transformation of metastable minerals, such as siderite into limonite and dissolution of anhydrite nodules (Alekseev *et al*., in press).

3. PALAEOGEOGRAPHIC CONTEXT

Available palaeogeographic reconstructions show a westerly siliciclastic source for Oka time and shifts to a more southerly source during the Tarusian (Fig. 3; Osipova and Belskaya, 1966; Birina *et al*., 1971; Belskaya *et al*., 1975). These reconstructions were based mainly on field lithology (laterally changing proportion of sandstones, siltstones, shales, and carbonates) with apparently no geochemical or detrital mineral data used. The southern potential sourceland of the Voronezh High is a Precambrian crystalline massif (Fig. 2) composed of longitudinally trending blocks of gneiss, granite, and greenstone composition with important banded iron formations (BIFs or ferrous quartzites of the Kursk Magnetic Anomaly; Gusel'nikov, 1981; Shchipansky and Bogdanova, 1996; Dagelaysky, 1997; Shevyrev *et al*., 2004; Bekker *et al*., 2010). Makhlina *et al*. (1993) developed early ideas about the submerged Voronezh High and the united Moscow–Donets Basin established during Oka time (Novik and Brazhnikova, 1949; Shvetsov, 1938; Tikhiy, 1941). According to Makhlina *et al*. (1993), the Voronezh High became completely submerged during the Venevian. This reconstruction was based on the similarity of sedimentary successions and marine fossil assemblages north and south of the Voronezh High, as well as a lack of evidence for sourceland proximity in carbonate-dominated Viséan–Serpukhovian sections of its southern (Dnieper–Donets Basin) slope. However, Carboniferous rocks are absent on a broad area of the central and northern Voronezh High. In the central, hypsometrically highest part of the Voronezh High (Fig. 2), the Precambrian basement is only covered by thin (20–50 m) Devonian volcaniclastics and proximal siliciclastics. An unconformity at the top of the Devonian is imprinted by a mature weathering crust and onlapped with erosion by Cretaceous sandstones and chalk (Shatsky and Mushenko, 1949; Shevyrev *et al*., 2004; unpublished data of the authors). Existence of this unconformity is more

DOI: 10.1002/gj

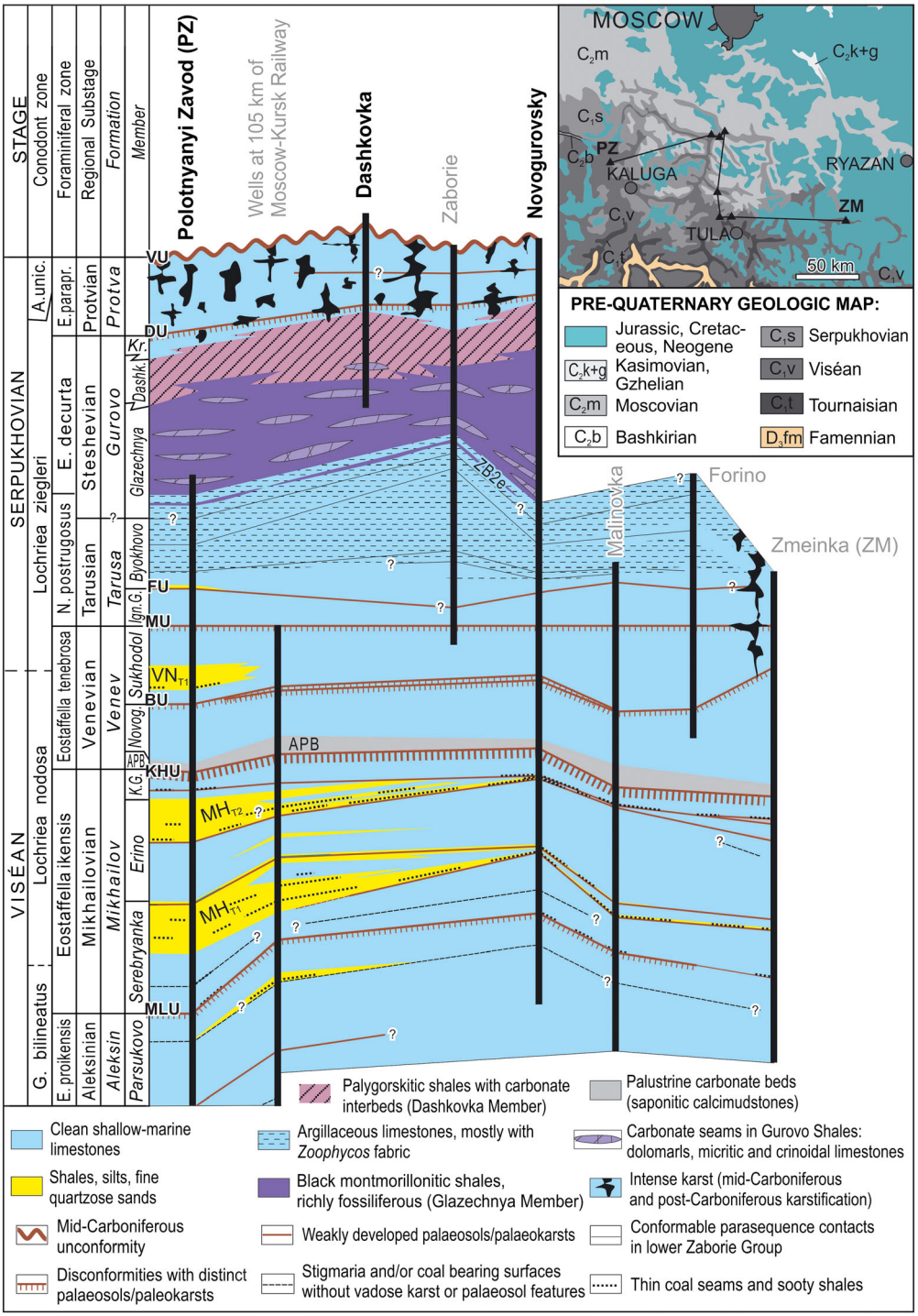

Figure 1. Stratigraphic framework and simplified cross-section of the upper Viséan–Serpukhovian succession of southern Moscow Basin (PZ-ZM line on map) (modified from Alekseev *et al*., in press). Sections with geochemical data used in this paper are named in bold; other sections in grey. Foraminiferal and conodont zones as shown in Kabanov *et al*. (2014). Abbreviated zone names: *G. bilineatus* is *Gnathodus bilineatus*, *A. unic*. is *Adetognathus unicornis*, *E. proikensis* is *Eostaffella proikensis*, *A. gigas* is *Archaediscus gigas*, *N. postrugosus* is *Neoarchaediscus postrugosus*, *P. globosa is Pseudoendothyra globosa*, *E. decurta* is *Eostaffellina decurta*, and *E. parapr*. is *Eostaffella paraprotvae*. Members of the Aleksin and Mikhailov formations are retained from Makhlina *et al*. (1993), and members of the Venev–Gurovo interval as updated in Kabanov *et al*. (2014). Member abbreviations: K.G. is Kumova Gora, APB is Akulshino, Novog. is Novogurovsky, Ign.G. is Ignatova Gora, Dashk. is Dashkovka, and Kr. is Kremenskoe. Names of main disconformities (in bold letters on left edge of the cross-section): MLU is Malinovka, KHU is Kholm, BU is Barsuki, MU is Muratovka, FU is Forino, DU is Dashkovka, and VU is Vysokoe (also known as mid-Carboniferous unconformity). Labelling of Oka siliciclastic wedges: MH_{T1} is lower Mikhailov, MH_{T1} is upper Mikhailov, and VN_{T1} is Venev. Inset map: trace of the PZ-ZM cross-section placed on Pre-Quaternary geological map of Russia 1:2500k. This figure is available in colour online at wileyonlinelibrary.com/journal/gj

DOI: 10.1002/gj

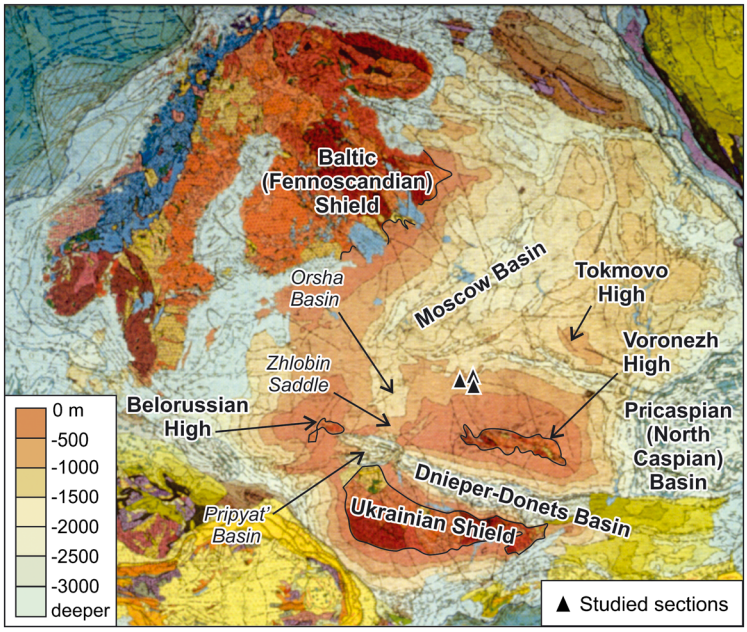

Figure 2. Surface of Archaean–Lower Proterozoic crystalline basement of the East European Craton (EEC) on the IUGS Tectonic Map of Europe 1:5 000 000 (1975). Structures discussed in this paper are indicated in bold (major structures) and italics (smaller-scale structures). Zero (sea level) isohypse is traced by the black line within the limits of the EEC. Geological information for basement is drawn only above sea level. This figure is available in colour online at wileyonlinelibrary.com/journal/gj

consistent with reconstruction of the Voronezh Land as persisting throughout the Carboniferous (Osipova and Belskaya, 1966; Birina *et al*., 1971; Belskaya *et al*., 1975). Palaeontological similarity of the two basins can be a result of their broad connection through the Volga–Uralian epeiric seaway to the east of the Voronezh High (see maps in Nikishin *et al*., 1996) and maybe also through the Pripyat' Basin along the western margin of the Voronezh Land (Fig. 2; Akimets *et al*., 1971).

The western provenance proposed for the Oka Group (Fig. 3A) is poorly constrained in the literature, mostly referred to as 'the inferred land' (Belskaya *et al*., 1975; Birina *et al*., 1971; Makhlina *et al*., 1993). It is generally connected to a broad area spanning the Belorussian High and the Baltic (Fennoscandian) Shield (Fig. 2) where the Mississippian is absent. Remobilization of siliciclastics could also proceed over uplifted Lower Palaeozoic basins of the western EEC. Within this area, the Zhlobin Saddle and Orsha Basin of eastern Belarus and westernmost Russia were geographically closest to the studied sections (Fig. 2). Palaeogeographic reconstructions depict these areas as mostly subaerially exposed and being actively eroded during the upper half of the Mississippian, although they could have been partly flooded during Oka time (Akimets *et al*., 1971). The Precambrian basement of the Belorussian High is strongly dominated by gneisses and felsic intrusives with very few ores (Pap, 1971). The eastern Fennoscandian Shield is dominated by felsic blocks with subordinate greenstones and relatively rare mafic intrusions (Hölttä *et al*., 2008; Lahtinen, 2012; Lauri *et al*., 2012).

4. MATERIALS AND METHODS

The Polotnyanyi Zavod section (54°43′N, 35°58′E) was measured and sampled for geochemistry in 2012 (Alekseev *et al*., in press; Kabanov *et al*., 2014). The stratigraphic density of sampling is shown in Figure 4 (116 samples in total), and sample numbers and elemental values are given in Appendix 1. The Oka Group of the section Novogurovsky (54°29′N, 37°19′E) was sampled for geochemistry in 2013 (Fig. 5; 80 samples in total), and XRF data are available in Appendix 2 (Supporting Information). XRF data from Novogurovsky have not been published before. The Lower Serpukhovian section of Novogurovsky was sampled in 2009 (Fig. 6; Kabanov *et al*., 2012). These samples from 2009 have been mostly collected for conodonts from 10–20 cm-thick stratigraphic intervals. These averaged samples were used for XRF and XRD analyses presented in Kabanov *et al*. (2012). Smaller-sized chip samples 26, 27-1, and 27-2 were taken from another sample set collected for the study of the Forino Unconformity. Chip samples

DOI: 10.1002/gj

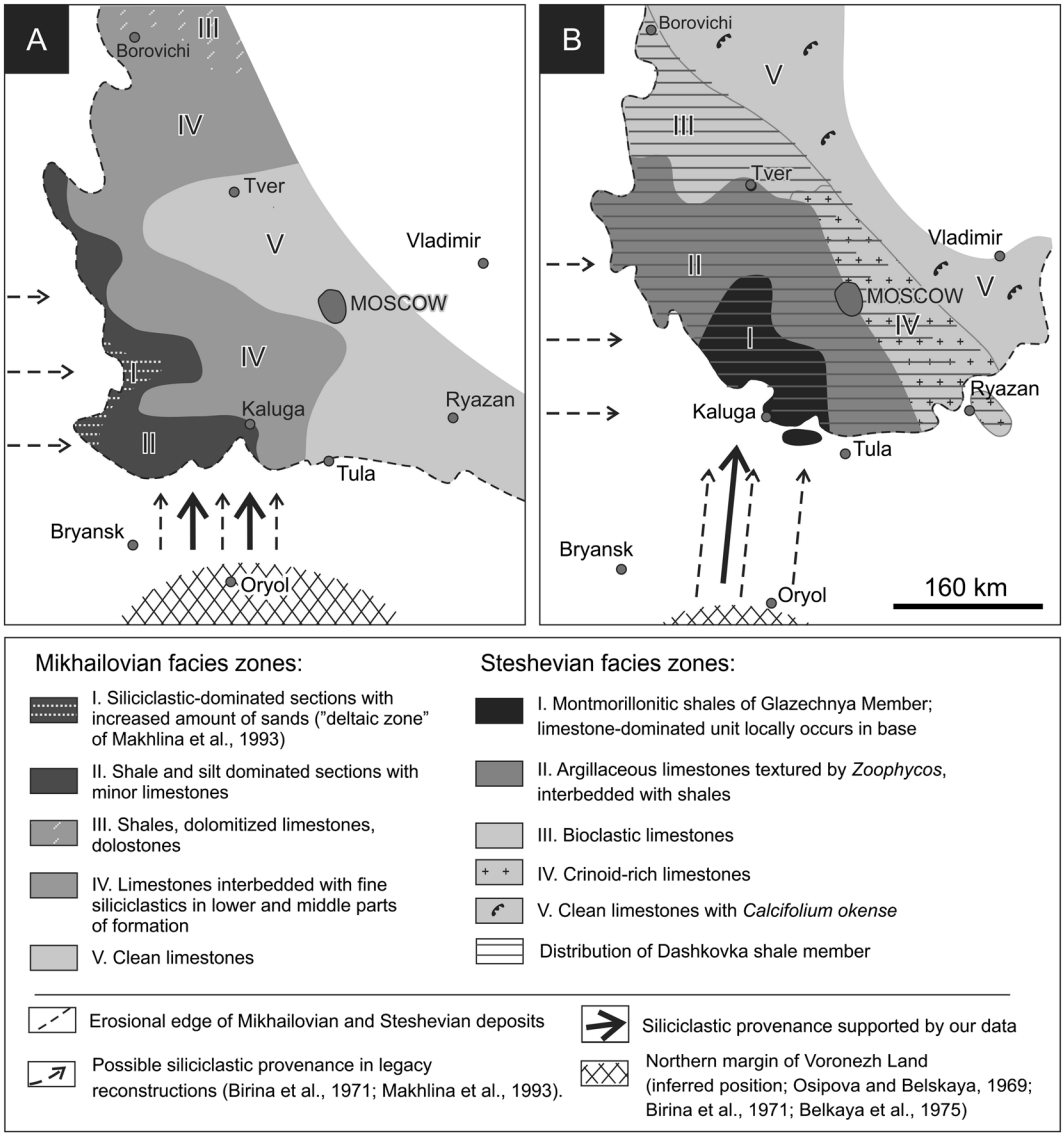

Figure 3. Facies zones and palaeogeography of Moscow Basin showing inferred siliciclastic sourcing (based on maps in Makhlina *et al*., 1993): (**A**) Mikhailovian (Upper Viséan); (**B**) Steshevian (Lower Serpukhovian).

from Dashkovka Quarry (54°54′N, 37°19′E) were collected in 2006 (Kabanov *et al*., 2012). Geographic coordinates of all three sections are given in the World Geodetic System WGS84 reference.

Bulk-rock geochemical data were obtained with the desktop WD-XRF crystal diffraction scanning spectrometer 'SPECTROSCAN MAKC-GV' at the ISSP RAS facility in Pushchino, Russia. The hand samples, 150–200 g each, were collected from the least weathered patches of Polotnyanyi Zavod and Novogurovsky sections (Figs. 5 and 6; Appendix 2). The sample preparation included drying and grinding of the rock to the particle size about 50 μm and pressing into pellets for measurement. Counts per second were converted to % or ppm. Limits of detection for most elements were from 5 ppm, for the light-end elements less precise (0.5% for Na and 0.02% for Mg). The quantitative analysis was based upon 24 standard rock and soil calibration samples.

In addition, magnetic susceptibility (MS) was measured using KLY-2 Kappabridge device in the same set of 116 samples collected from Polotnyanyi Zavod (Alekseev *et al*., in press). Three measurements were made on each sample, weighed with a precision of 0.01 g. Data were normalized on mass-specific MS expressed in $m^3\,kg^{-1} \times 10^{-8}$. The dimensionless δMS notation for magnetic susceptibility data is used here and in Alekseev *et al*. (in press). $\delta MS = (MS_{measured} - MS_{marine\ standard})/MS_{marine\ standard}$. The MS marine standard of $5.5\,m^3\,kg^{-1} \times 10^{-8}$ is used as the median value for lithified marine sedimentary rocks (Ellwood *et al*., 2011).

DOI: 10.1002/gj

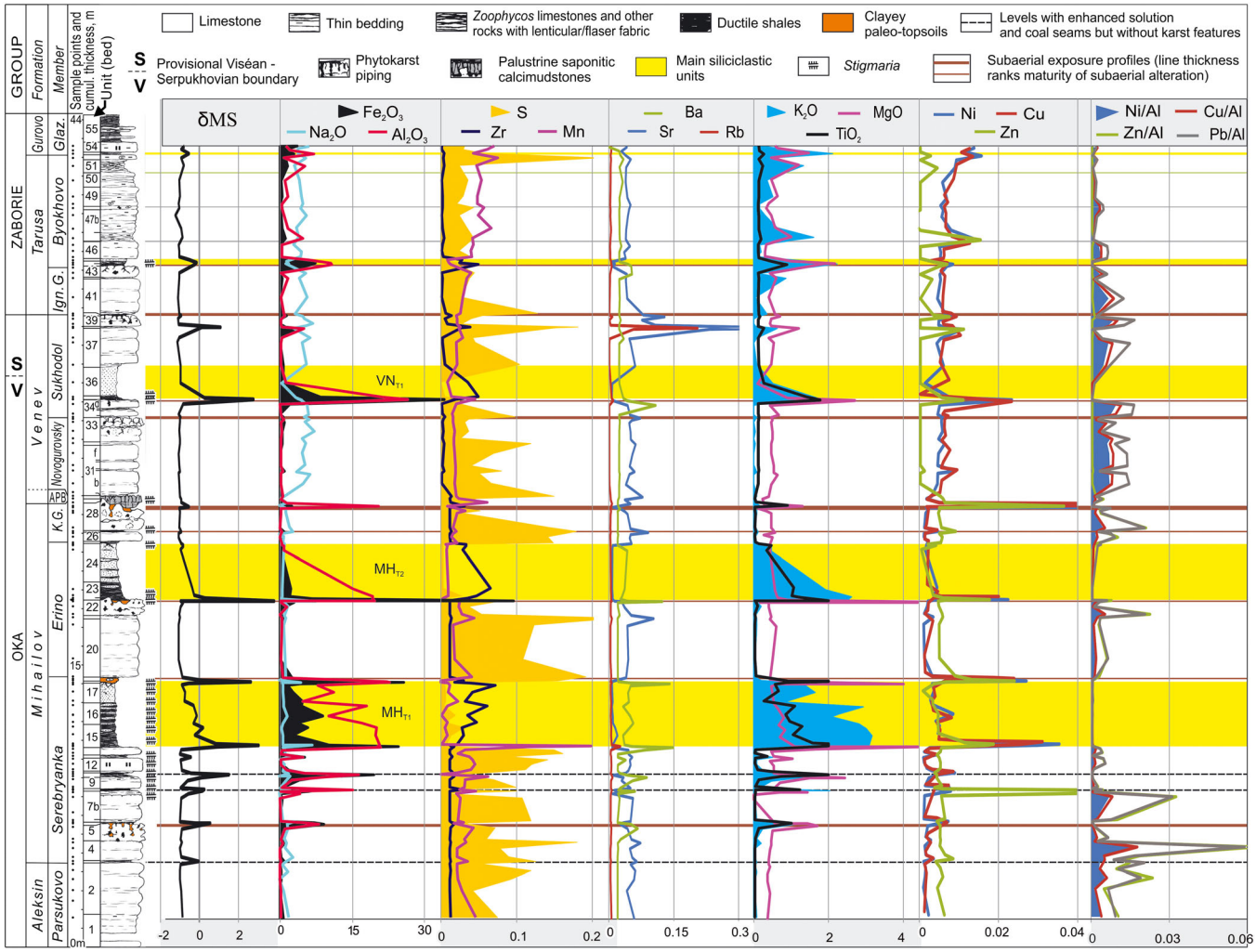

Figure 4. Bulk geochemical and magnetic susceptibility logs for section Polotnyanyi Zavod (section description is given in Kabanov *et al.*, 2014). This figure is available in colour online at wileyonlinelibrary.com/journal/gj

5. GEOCHEMISTRY RESULTS OF THE OKA GROUP

5.1. Main elements

Limestones and siliciclastic beds in both the Polotnyanyi Zavod and Novogurovsky sections are strikingly expressed on the bulk geochemical logs, although in the latter section siliciclastic wedges pinch into thin (under 10–15 cm) seams in the Mikhailov Formation and completely disappear in the Venev Formation (Figs. 4 and 5).

The basic analysis of element abundance in the Aleksin–Venev succession screens elements that are usual for this sedimentary system from those that are rare or exotic (Fig. 7A, B). The cutoff is chosen at 0.1% of truncated average (interquartile mean or IQM in Fig. 7). Of the usual elements, the major or rock-forming ones are Ca, Si, Al, and Na, and in Polotnyanyi Zavod these are joined by Fe (Fig. 4). Sodium shows an interesting stratigraphic inversion in Polotnyanyi Zavod. The Aleksin–Mikhailov limestones there are Na-lean with low peaks in siliciclastic beds. In the Venev Formation, the background Na_2O value of limestones shifts from 1.5% to 4.5%, whereas disconformity-associated siliciclastics-enriched horizons become depleted in sodium. However, the Oka section of Novogurovsky shows higher Na values in limestones than in siliciclastic seams (Fig. 5).

Other usual elements with IQM exceeding or approaching 0.1% and locally exceeding 1% are Mg, K, and Ti (Fig. 7). Titanium is relatively abundant in the siliciclastic wedges (Ti up to 2.3% in Polotnyanyi Zavod and up to 0.52% in Novogurovsky). However, clean sandstones tend to be iron lean and also depleted in most siliciclastic-associated elements, except maybe for zirconium (Fig. 4; Alekseev *et al.*, in press). Mg in the Oka Group stays at a low background value of 0.5% (attesting to a lack of dolomite) but gives spikes up to 3.4% at the same levels as iron and MS where it appears to be bound in clay minerals (Fig. 4). Potassium,

DOI: 10.1002/gj

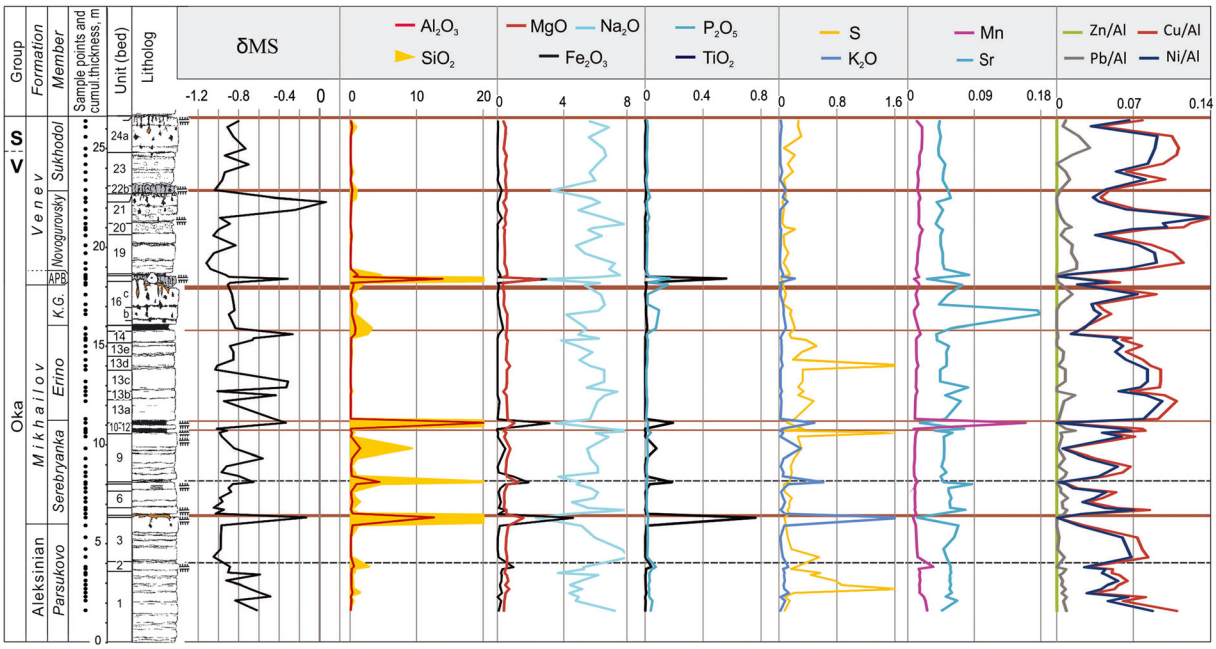

Figure 5. Bulk geochemical and magnetic susceptibility logs for the Oka Group of section Novogurovsky (section description is given in Kabanov *et al*., 2012). This figure is available in colour online at wileyonlinelibrary.com/journal/gj

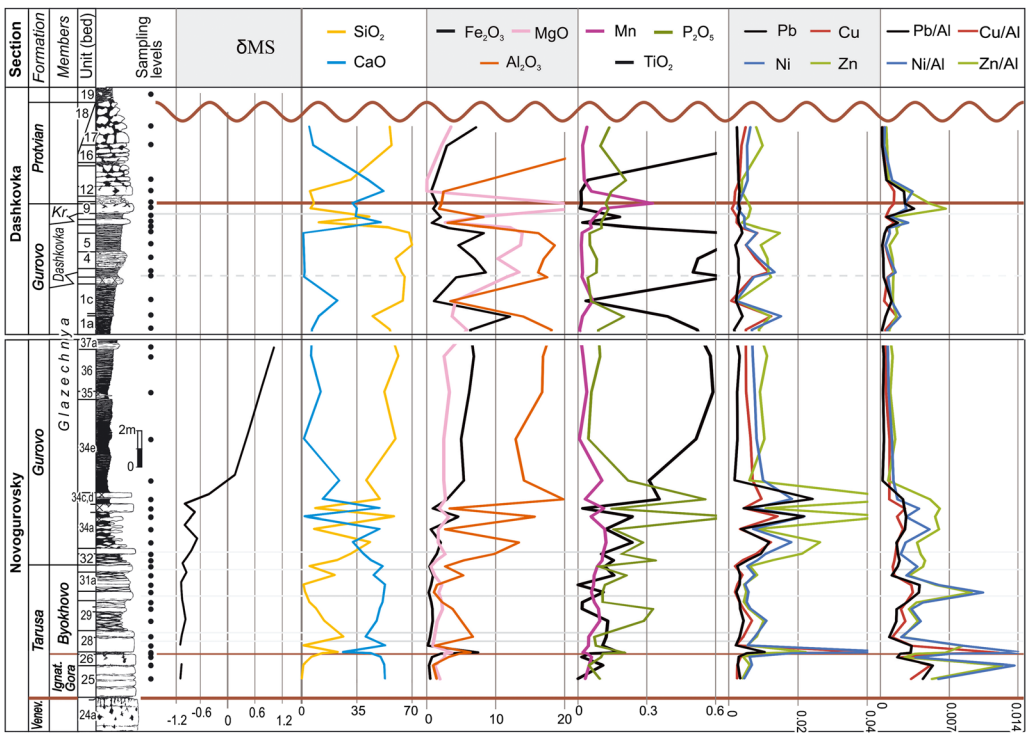

Figure 6. Bulk geochemical and magnetic susceptibility logs for the Serpukhovian Stage of combined section Novogurovsky and Dashkovka (both sections are described in Kabanov *et al*., 2012). This figure is available in colour online at wileyonlinelibrary.com/journal/gj

DOI: 10.1002/gj

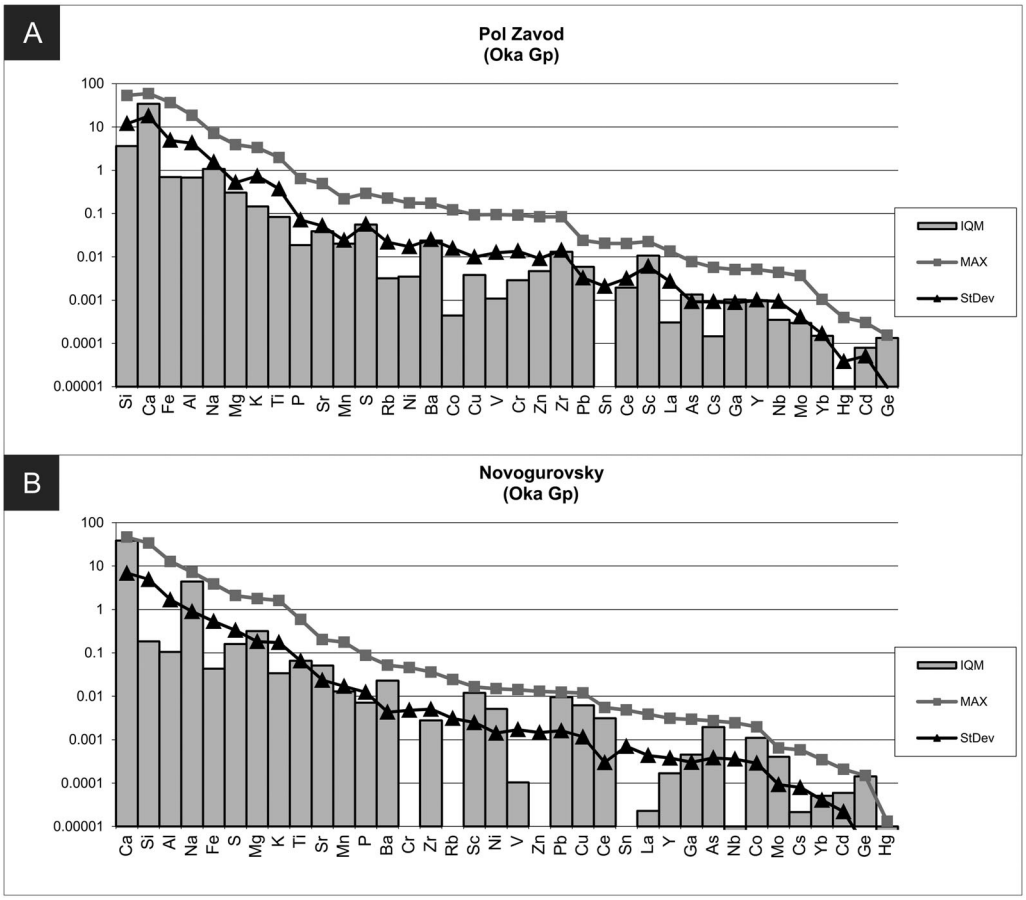

Figure 7. Basic analysis of dataset from the Oka Group: (**A**) Polotnyanyi Zavod and (**B**) Novogurovsky; IQM stands for the interquartile mean, MAX for greatest values, and StDev for the standard deviation. Data are sorted by greatest values.

unlike sodium, is clearly bound in fine siliciclastics, apparently micas (Figs. 4 and 5).

5.2. *Covariation of elements*

Correlation matrix of datasets from the Oka Group reveals two major groups of elements: limestone-associated ('calciphile') and siliciclastics-associated or 'silicophile' (Tables 1 and 2). Of the major elements, only sodium persistently associates with Ca in marine limestones. Sulphur also resides preferentially in limestones (Pearson r (Ca, S) = 0.6 in Polotnyanyi Zavod and 0.1 in Novogurovsky) where it probably occurs in the form of finely disseminated pyrite and possibly some gypsum. Of the minor elements reaching or exceeding concentrations of 0.1%, only Sr resides predominantly in limestones (Pearson r (Ca, Sr) = 0.43 in Polotnyanyi Zavod and 0.31 in Novogurovsky). Scandium is a strongly calciphile rare earth element persisting in limestones at very stable background values of 0.01–0.02% and diminishing by one magnitude, sometimes to zero, in siliciclastic beds (Pearson r (Ca, Sc) = 0.89 in both sections).

The siliciclastic association is strongly expressed by Al, Si, Ti, Zr, Fe, Mg, and K bundled by strong covariation (Pearson r exceeding 0.6 in Tables 1 and 2). Most of these elements preferentially reside in finer-grained, aluminosilicate-rich parts of siliciclastic units (Fig. 4). Clean sandstones are somewhat depleted in most elements of siliciclastic association, except for SiO_2 (quartz sand itself) and Zr bound in detrital zircon grains (Fig. 4).

5.3. *Manganese and trace metals*

Manganese and a number of trace metals forming sulphides in sulphate-reducing sedimentary conditions (referred to as sulphidophile metals by Kabanov *et al.*, 2012 and Alekseev *et al.*, in press) are discussed together because they are frequently utilized as valuable indicators of redox regime and anoxia (Algeo and Maynard, 2004; Calvert and Pedersen, 1993; Harris *et al.*, 2013). Trace metals that are present in the Oka and Zaborie groups in appreciable quantities and show enrichment horizons include Cu, Ni, Zn, Pb, Co, and Cr, and the first four of these elements shown on the logs (Figs. 4–6) are discussed in more detail below. Concentrations of these

DOI: 10.1002/gj

Table 1. Pearson *r* correlation matrix of magnetic susceptibility (MS) and elements in the Oka Group of Polotnyanyi Zavod

	MS	Si	Ca	Fe	Al	Na	Mg	K	Ti	P	Sr	Mn	S	Rb	Ni	Ba	Co	Cu	V	Cr	Zn	Zr	Pb	Sn	Ce	Sc	La
MS	1.00																										
Si	0.45	1.00																									
Ca	-0.55	-0.91	1.00																								
Fe	0.94	0.40	-0.50	1.00																							
Al	0.74	0.79	-0.82	0.68	1.00																						
Na	0.20	-0.28	0.21	0.23	-0.11	1.00																					
Mg	0.91	0.33	-0.42	0.94	0.62	0.31	1.00																				
K	0.52	0.85	-0.77	0.43	0.83	-0.21	0.38	1.00																			
Ti	0.87	0.71	-0.76	0.82	0.91	0.06	0.81	0.77	1.00																		
P	0.29	0.04	-0.04	0.15	0.07	0.17	0.16	0.07	0.09	1.00																	
Sr	-0.05	-0.40	0.43	-0.22	-0.36	0.28	-0.17	-0.34	-0.34	0.69	1.00																
Mn	0.26	-0.13	0.12	0.21	0.03	0.13	0.30	0.00	0.17	0.14	0.04	1.00															
S	-0.23	-0.57	0.60	-0.25	-0.44	-0.06	-0.20	-0.49	-0.44	0.21	0.52	0.10	1.00														
Rb	0.28	-0.01	0.01	0.05	0.01	0.15	0.06	0.01	0.04	0.70	0.84	0.12	0.23	1.00													
Ni	0.30	0.22	-0.31	0.28	0.44	0.02	0.35	0.10	0.37	0.06	-0.11	0.10	-0.18	0.04	1.00												
Ba	0.91	0.53	-0.61	0.91	0.73	0.20	0.92	0.54	0.91	0.13	-0.27	0.31	-0.35	0.05	0.28	1.00											
Co	0.82	0.21	-0.36	0.88	0.47	0.37	0.91	0.25	0.67	0.12	-0.15	0.39	-0.19	0.06	0.26	0.83	1.00										
Cu	0.45	0.26	-0.37	0.43	0.53	0.15	0.50	0.17	0.50	0.13	-0.09	0.18	-0.20	0.08	0.97	0.45	0.41	1.00									
V	0.88	0.48	-0.57	0.86	0.77	0.14	0.84	0.53	0.89	0.13	-0.24	0.14	-0.28	0.04	0.33	0.91	0.71	0.48	1.00								
Cr	0.75	0.38	-0.58	0.73	0.61	0.04	0.67	0.39	0.69	0.07	-0.27	0.14	-0.29	0.02	0.21	0.76	0.63	0.31	0.78	1.00							
Zn	0.31	0.09	-0.32	0.27	0.31	-0.21	0.27	0.07	0.26	0.04	-0.16	0.14	-0.10	0.00	0.47	0.27	0.28	0.45	0.30	0.71	1.00						
Zr	0.23	0.82	-0.74	0.12	0.58	-0.42	0.05	0.66	0.42	0.13	-0.14	-0.22	-0.34	0.20	0.11	0.23	-0.01	0.10	0.23	0.17	0.04	1.00					
Pb	-0.20	-0.37	0.16	-0.16	-0.36	0.44	-0.08	-0.57	-0.31	0.00	0.17	-0.20	0.04	0.02	0.15	-0.15	0.02	0.14	-0.19	0.11	0.33	-0.34	1.00				
Sn	0.27	0.14	-0.37	0.23	0.24	-0.05	0.18	0.06	0.22	-0.02	-0.17	0.05	-0.23	0.00	0.24	0.25	0.24	0.24	0.27	0.75	0.89	0.04	0.43	1.00			
Ce	0.66	0.64	-0.67	0.62	0.80	0.24	0.51	0.74	0.79	0.20	-0.20	0.06	-0.45	0.09	0.19	0.67	0.45	0.35	0.75	0.54	0.06	0.40	-0.31	0.15	1.00		
Sc	-0.45	-0.88	0.89	-0.39	-0.71	0.09	-0.33	-0.70	-0.63	-0.09	0.32	0.20	0.60	-0.04	-0.27	-0.49	-0.21	-0.31	-0.40	-0.43	-0.20	-0.69	0.06	-0.29	-0.58	1.00	
La	0.75	0.68	-0.74	0.71	0.89	-0.04	0.64	0.79	0.88	0.09	-0.34	0.08	-0.34	0.01	0.24	0.75	0.57	0.38	0.79	0.62	0.24	0.44	-0.33	0.19	0.82	-0.57	1.00

The elements are recalculated from oxides and sorted by greatest values (original data in Appendix 1). Elements with greatest values below 10 ppm are excluded.

elements are normalized to Al (Figs. 4 and 5), which is a conventional correction for clay input (Algeo and Maynard, 2004; Calvert and Pedersen, 1993).

The logs in sections of the Oka Group (Figs. 4 and 5) show that Cu essentially repeats the distribution of Ni, forming a Cu–Ni couple (also expressed in the strongest Cu–Ni covariation in Tables 1 and 2) and indicating an essentially identical accumulation history of these two metals. Pb mimics the distribution of Zn in the Aleksin–Mikhailov interval of Polotnyanyi Zavod, but in the younger part of the section Zn decouples from Pb (Fig. 4), and there is no Pb–Zn correlation in the Oka Group of Novogurovsky. Enrichment horizons of Cu, Ni, Zn, Pb, and also Cr and Co occur in the fine-grained bases of siliciclastic packages (Units 15, 23a, and 35 in Fig. 4) and thin shales capping palaeokarsts (Units 18–19 and 29 in Fig. 4). Cobalt in these horizons shows the sharpest spikes,

Table 2. Pearson *r* correlation matrix of MS and elements in the Oka Group of Novogurovsky

	MS	Ca	Si	Al	Na	Fe	S	Mg	K	Ti	Sr	Mn	P	Ba	Cr	Zr	Rb	Sc	Ni	V	Zn	Pb	Cu	Ce	Sn	La	Y	Ga	As	Nb	Co
MS	1.00																														
Ca	-0.45	1.00																													
Si	0.44	-0.98	1.00																												
Al	0.42	-0.97	0.95	1.00																											
Na	-0.34	0.49	-0.52	-0.48	1.00																										
Fe	0.42	-0.93	0.97	0.90	-0.55	1.00																									
S	-0.12	0.10	-0.12	-0.11	-0.03	-0.11	1.00																								
Mg	0.38	-0.81	0.85	0.75	-0.49	0.80	0.04	1.00																							
K	0.38	-0.75	0.82	0.66	-0.45	0.86	-0.06	0.58	1.00																						
Ti	0.42	-0.90	0.94	0.79	-0.50	0.92	-0.11	0.86	0.86	1.00																					
Sr	-0.22	0.31	-0.29	-0.29	0.06	-0.27	0.05	-0.20	-0.22	-0.27	1.00																				
Mn	0.22	-0.50	0.42	0.66	-0.19	0.40	-0.04	0.11	0.17	0.12	-0.22	1.00																			
P	0.09	-0.32	0.31	0.28	-0.31	0.28	-0.04	0.42	0.04	0.33	0.34	0.01	1.00																		
Ba	0.42	-0.92	0.97	0.86	-0.51	0.95	-0.12	0.90	0.82	0.97	-0.28	0.24	0.34	1.00																	
Cr	0.31	-0.72	0.72	0.66	-0.43	0.64	-0.10	0.88	0.32	0.75	-0.21	0.06	0.56	0.76	1.00																
Zr	0.33	-0.83	0.84	0.82	-0.48	0.83	-0.08	0.62	0.75	0.76	0.20	0.44	0.38	0.76	0.48	1.00															
Rb	0.06	-0.14	0.14	0.12	-0.14	0.15	-0.07	0.11	0.17	0.15	0.77	-0.01	0.41	0.11	0.06	0.55	1.00														
Sc	-0.41	0.89	-0.91	-0.90	0.45	-0.89	0.09	-0.76	-0.73	-0.82	0.17	-0.44	-0.30	-0.87	-0.63	-0.82	-0.20	1.00													
Ni	0.00	-0.28	0.29	0.23	-0.31	0.28	0.04	0.51	0.04	0.35	0.04	-0.11	0.66	0.37	0.63	0.19	0.08	-0.25	1.00												
V	0.39	-0.86	0.92	0.76	-0.51	0.92	-0.08	0.81	0.90	0.98	-0.27	0.11	0.28	0.94	0.66	0.75	0.13	-0.81	0.35	1.00											
Zn	0.37	-0.85	0.84	0.79	-0.45	0.75	-0.11	0.90	0.46	0.84	-0.25	0.19	0.52	0.84	0.97	0.62	0.10	-0.74	0.54	0.76	1.00										
Pb	-0.55	0.47	-0.50	-0.39	0.21	-0.52	0.09	-0.29	-0.67	-0.55	0.10	-0.08	0.02	-0.48	-0.16	-0.50	-0.23	0.42	0.06	-0.56	-0.27	1.00									
Cu	-0.22	0.12	-0.11	-0.17	-0.14	-0.10	0.10	0.17	-0.25	-0.02	0.25	-0.29	0.58	-0.02	0.31	-0.10	0.11	0.10	0.89	0.01	0.19	0.28	1.00								
Ce	0.41	-0.91	0.95	0.86	-0.54	0.98	-0.11	0.74	0.92	0.93	-0.24	0.35	0.27	0.93	0.57	0.85	0.19	-0.87	0.23	0.94	0.71	-0.56	-0.13	1.00							
Sn	0.43	-0.98	0.94	0.98	-0.48	0.88	-0.11	0.77	0.63	0.82	-0.31	0.59	0.33	0.85	0.75	0.81	0.13	-0.87	0.28	0.77	0.87	-0.39	-0.11	0.85	1.00						
La	0.31	-0.70	0.75	0.59	-0.45	0.77	-0.10	0.52	0.89	0.82	-0.25	0.09	0.23	0.76	0.36	0.66	0.10	-0.64	0.05	0.83	0.49	-0.55	-0.22	0.86	0.59	1.00					
Y	0.28	-0.75	0.78	0.65	-0.39	0.77	0.00	0.60	0.79	0.81	-0.28	0.17	0.35	0.77	0.48	0.65	0.04	-0.67	0.23	0.83	0.59	-0.52	-0.06	0.83	0.66	0.87	1.00				
Ga	0.40	-0.93	0.90	0.99	-0.45	0.85	-0.12	0.69	0.60	0.71	-0.30	0.74	0.24	0.80	0.60	0.78	0.09	-0.86	0.17	0.67	0.73	-0.34	-0.21	0.80	0.95	0.53	0.59	1.00			
As	-0.37	0.28	-0.31	-0.22	0.11	-0.33	0.15	-0.16	-0.48	-0.37	-0.24	0.06	-0.03	-0.30	-0.07	-0.48	-0.50	0.28	0.04	-0.39	-0.15	0.83	0.19	-0.37	-0.22	-0.35	-0.32	-0.18	1.00		
Nb	0.39	-0.70	0.73	0.60	-0.32	0.70	-0.11	0.62	0.68	0.79	-0.57	0.10	0.12	0.75	0.58	0.42	-0.16	-0.60	0.18	0.77	0.66	-0.47	-0.15	0.72	0.65	0.73	0.70	0.55	-0.21	1.00	
Co	-0.32	0.64	-0.63	-0.65	0.32	-0.59	-0.03	-0.53	-0.42	-0.54	0.24	-0.43	-0.27	-0.57	-0.50	-0.51	-0.02	0.64	-0.22	-0.50	-0.58	0.20	-0.02	-0.59	-0.66	-0.40	-0.42	-0.63	-0.13	-0.41	1.00

The elements are recalculated from oxides and sorted by greatest values (original data in Appendix 2). Elements with greatest values below 10 ppm are excluded.

DOI: 10.1002/gj

from essentially zero in the vast majority of samples to 0.1% (Appendix 1). These metal enrichment horizons (abbreviated as MEHs in this paper) also stand out by the high spikes of magnetic susceptibility and the high iron content (Fig. 4) in the form of secondary goethite and some residual siderite (Alekseev *et al*., in press). The alumina content also reaches its highest values in MEHs, which on Al-normalized logs is expressed by the elimination of trace-metal spikes (Figs. 4 and 5). In the Oka section of Novogurovsky, trace-metal enrichment horizons are less distinct, and almost unrecognizable. Noteworthy is the average content of Pb and Zn, which falls by one order from Polotnyanyi Zavod (0.006% for both elements) to Novogurovsky (0.0003% for Zn and 0.0006% for Pb), whereas the average content of the Cu–Ni couple remains unchanged (0.005–0.007% for each element; see Appendices 1 and 2).

Manganese behaves differently from trace metals. In both sections the Mn curve mostly stays featureless, at low background values of 0.013–0.02% (Figs. 4 and 5). However, in the base of Unit 15 of Polotnyanyi Zavod, Mn peaks at 0.25% (Fig. 4). In Novogurovsky, similar Mn enrichment is encountered in a sample from Unit 12 (Fig. 5). Both Mn-rich horizons occur at very close stratigraphic levels (Unit 12 of Novogurovsky and Unit 15 of Polotnyanyi Zavod), both within the siliciclastic unit MH_{T1} in similar sediments—sooty shales with extensive *Stigmaria* penetrations, although in Novogurovsky this unit is much thinner (Figs. 1, 4, and 5).

Noteworthy are palaeokarsts, which formed in well-drained vadose environments, that mostly have signatures of iron and trace metals close to background of non-karstified limestones (Figs. 4 and 5; Alekseeva *et al*., 2012; Alekseev *et al*., in press). The Akulshino palustrine marl (APB unit in Figs. 4 and 5) is a siliciclastic-lean deposit, which generally does not show enrichment in Fe and trace metals (Alekseev *et al*., in press; Alekseeva *et al*., 2012). Out of the four samples taken from the APB bed in Novogurovsky, only one shows a spike in Fe, Ti, and MS (Fig. 5). This sample (NG-17fill in Appendix 2) is a siliciclastic-rich infill of a solution pocket and is probably not part of a typical saponitic palustrine facies. In Polotnyanyi Zavod, the APB unit shows a low MS spike and corresponding spike in iron in its basal, siliciclastic-enriched part (sample PZ-30 in Appendix 1). This sample is also enriched in clay (high Al_2O_3), Cu, Ni, and Zn (Fig. 4).

5.4. Strontium and rubidium

Strontium occurs in trace quantities predominantly in limestones. Rubidium is generally alien to this sedimentary system—it is virtually absent in the Oka and Zaborie limestones and rises to only 0.05% in some siliciclastic-rich beds. However, the thin shale of Unit 38 of Polotnyanyi Zavod (upper Venev) is enriched in Rb (IQM up to 0.2%) and Sr (IQM up to 0.45%). Other signatures such as elevated TiO_2, Fe_2O_3, and Zr, a spike in MS, and admixture of quartz grains are in common with other beds rich in siliciclastic fines. The clay matrix in this shale has montmorillonite–beidellite composition and very light $\delta^{13}C$ of carbonate components (−9.46‰ in bulk samples and −11.93‰ in the mud fraction; Alekseev *et al*., in press). Unlike many shales blanketing disconformities, this shale is not associated with a morphologically distinct subaerial exposure surface.

One possible interpretation of the abnormally high Sr and Rb values in Unit 38 of Polotnyanyi Zavod is a likely volcanogenic component. In Novogurovsky this horizon has not been detected, either because of its genuine absence or because it was overlooked during section measurement and overstepped during sampling.

5.5. Magnetic susceptibility (MS)

The MS signal is generally stronger in Polotnyanyi Zavod (δMS −1.1 to 3.8) than in Novogurovsky (−1.1 to 0.06). In Polotnyanyi Zavod, MS shows the strongest correlation to bulk iron (Pearson $r = 0.94$; Table 1). In most cases both high MS and iron reside in finer-grained parts of siliciclastic units (Fig. 4), which is also expressed in good correlations of MS with Al_2O_3, MgO, and TiO_2 (Table 1). In the Oka Group of Novogurovsky with its wedging out siliciclastic beds, MS also shows the strongest covariation with iron, along with silica and titanium (Pearson *r* equals 0.42 for all three elements; Table 2). Limestones in both sections tend to be weakly paramagnetic to weakly diamagnetic with δMS fluctuating very close to −1 (Figs. 2 and 3). Calcium and MS correlate accordingly with maximum negative values (Pearson *r* (MS, Ca) = −0.55 in Polotnyanyi Zavod and −0.45 in Novogurovsky; Tables 1 and 2).

6. GEOCHEMISTRY RESULTS OF THE ZABORIE GROUP

6.1. Main elements and magnetic susceptibility

In the Zaborie Group part of the studied sections, curves of SiO_2, CaO, and Al_2O_3 show alternation of limestones and shales (Figs. 4 and 6). Other usual elements with the IQM concentrations exceeding 0.1% are Fe, Al, Mg, Na, and K in the lower Zaborie Group (Fig. 8A and 8B). In the upper Zaborie shales, these elements are joined by Ti (Fig. 8C). The background concentration of Mg (referred to here as IQM) increases significantly in the transition from the Glazechnya Shale (1.3%) to the Dashkovka Shale (7.3%), which is a signature of transition from montmorillonites to Mg-rich palygorskitic shale (Kabanov *et al*., 2012). Increase of Na^+ and K^+ from the carbonate-dominated upper Tarusa into the Glazechnya Shale is attributed to

DOI: 10.1002/gj

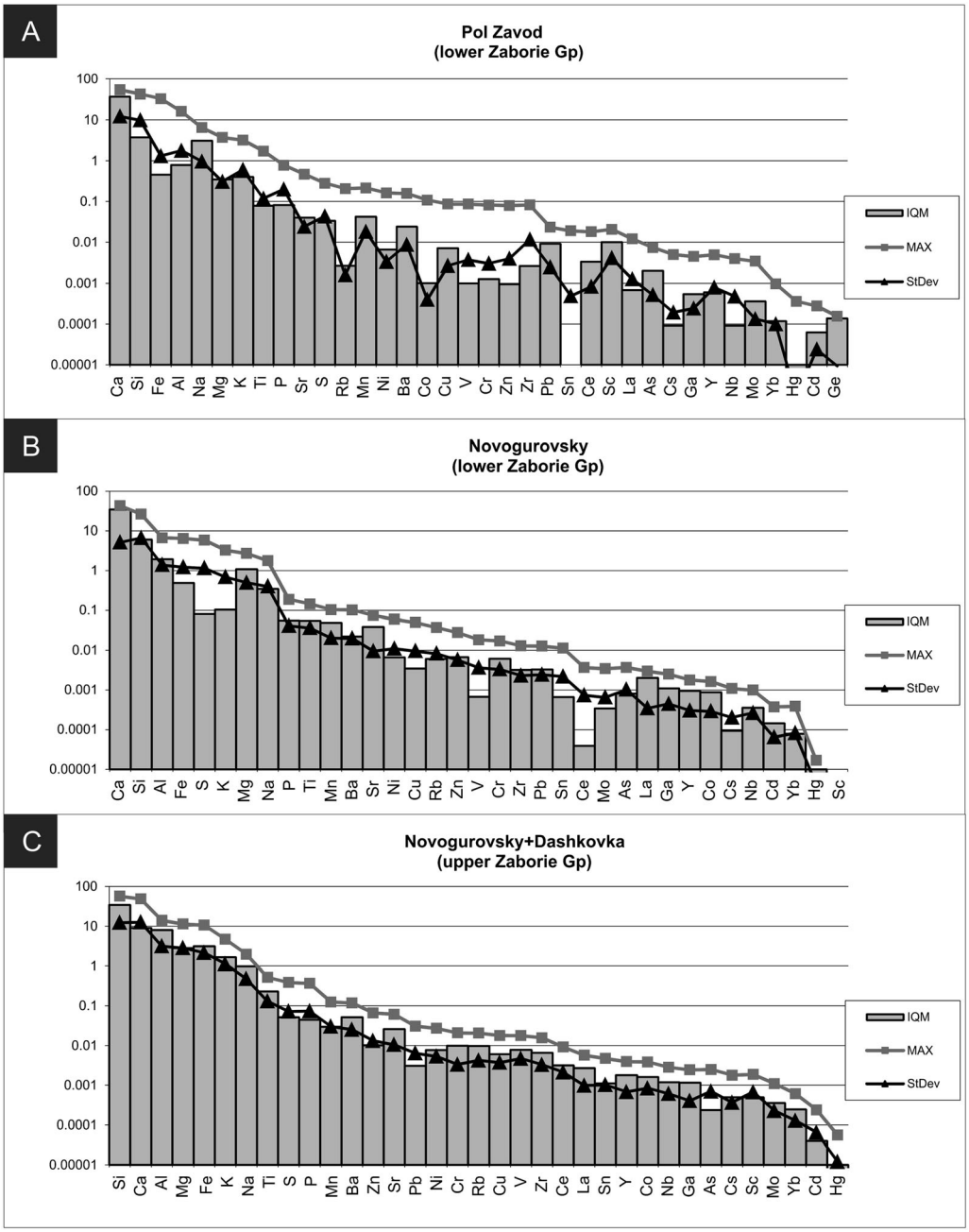

Figure 8. Basic analysis of dataset from the Zaborie Group: (**A**) Tarusa-basal Gurovo of Polotnyanyi Zavod (Units 40–54), (**B**) Tarusa-basal Gurovo of Novogurovsky (Units 25–32), and (**C**) Glazechnya and Dashkovka shale members from combined Novogurovsky + Dashkovka dataset; IQM stands for the interquartile mean, MAX for greatest values, and StDev for the standard deviation. Data are sorted by greatest values.

increasing fixation of these elements in clay minerals (Kabanov *et al.*, 2012). The upper part of the Glazechnya Shale is also distinctive for the elevated iron content in ferrimagnetic form, as indicated by high δMS exceeding the threshold of 0 (Fig. 6). Unfortunately, no MS data are available from the Dashkovka samples. The Glazechnya and Dashkovka Shales show a relatively high content of titanium reaching 0.4%. These values are markedly higher than concentrations of Ti in *Zoophycos*-bearing argillaceous limestones and shales of the Tarusa and basal Gurovo (Fig. 6) and are very close to the range of finer-grained siliciclastics of the Mikhailov and Venev formations in Polotnyanyi Zavod where Ti attains 0.5–1.6% (0.8–2.7% of TiO_2; Fig. 4).

DOI: 10.1002/gj

6.2. *Covariation of elements*

In the Zaborie Group, Ca^{2+} does not show a steady association with any of the measured elements (Tables 3–5). The limestones in the Tarusa–lowermost Gurovo of Polotnyanyi Zavod are enriched in Na similar to the underlying Oka Group limestones (Table 3), but in Novogurovsky the limestones of the lower Zaborie Group are depleted in Na (Pearson r (Ca, Na) = −0.88; Table 4). The lower Zaborie limestones of Polotnyanyi Zavod are also similar to the Oka limestones in elevated Sr and Sc, but in Novogurovsky these two show negative correlation with Ca (Table 4). The limestone beds of the upper Steshevian shale-dominated member show enrichment in Sr and traces of Cd and As (maximum values below 50 ppm), whereas in the shales these elements are virtually absent. Manganese in the lower and upper Zaborie Group shows more steady enrichment in limestones than in the Oka Group, which is discussed below.

Table 3. Pearson r correlation matrix of MS and elements in the lower Zaborie Group of Polotnyanyi Zavod (Units 40–54 in Fig. 4)

	MS	Ca	Si	Al	Fe	Na	K	Mg	P	Ti	S	Sr	Mn	Ba	Zr	Ni	Zn	V	Sc	Cu	Pb
MS	1.00																				
Ca	-0.71	1.00																			
Si	0.92	-0.75	1.00																		
Al	0.96	-0.71	0.95	1.00																	
Fe	0.97	-0.64	0.86	0.92	1.00																
Na	-0.40	0.79	-0.46	-0.44	-0.28	1.00															
K	0.89	-0.66	0.93	0.97	0.82	-0.44	1.00														
Mg	0.94	-0.59	0.89	0.98	0.92	-0.32	0.93	1.00													
P	0.39	0.06	0.33	0.33	0.41	0.27	0.30	0.35	1.00												
Ti	0.93	-0.64	0.89	0.93	0.93	-0.34	0.83	0.91	0.40	1.00											
S	0.20	0.26	0.13	0.14	0.23	0.37	0.12	0.21	0.88	0.23	1.00										
Sr	-0.05	0.52	-0.11	-0.08	0.03	0.53	-0.14	0.05	0.41	0.03	0.61	1.00									
Mn	-0.23	0.67	-0.28	-0.27	-0.17	0.68	-0.21	-0.20	0.52	-0.25	0.45	0.29	1.00								
Ba	0.86	-0.55	0.86	0.89	0.85	-0.25	0.82	0.91	0.31	0.92	0.16	0.02	-0.21	1.00							
Zr	0.86	-0.62	0.85	0.84	0.87	-0.34	0.73	0.81	0.40	0.97	0.27	0.15	-0.31	0.85	1.00						
Ni	0.45	0.09	0.38	0.45	0.46	0.29	0.54	0.52	0.48	0.30	0.41	0.32	0.48	0.37	0.20	1.00					
Zn	0.61	-0.26	0.59	0.67	0.59	-0.15	0.67	0.68	0.39	0.60	0.36	0.40	-0.14	0.54	0.60	0.55	1.00				
V	0.95	-0.62	0.89	0.96	0.93	-0.35	0.90	0.95	0.40	0.95	0.24	0.09	-0.25	0.86	0.90	0.46	0.67	1.00			
Sc	-0.64	0.93	-0.69	-0.68	-0.55	0.80	-0.70	-0.58	0.08	-0.51	0.27	0.52	0.58	-0.49	-0.46	-0.09	-0.30	-0.56	1.00		
Cu	0.23	0.33	0.15	0.23	0.27	0.47	0.33	0.34	0.44	0.11	0.45	0.46	0.58	0.21	0.02	0.96	0.44	0.27	0.14	1.00	
Pb	-0.63	0.96	-0.63	-0.64	-0.57	0.76	-0.58	-0.53	0.10	-0.55	0.27	0.53	0.69	-0.42	-0.52	0.13	-0.22	-0.56	0.90	0.36	1.00

The elements are recalculated from oxides and sorted by greatest values (original data in Appendix 1). Elements with greatest values below 10 ppm are excluded.

Table 4. Pearson r correlation matrix of MS and elements in the lower Zaborie Group of Novogurovsky (Units 25–32 in Fig. 6)

	MS	Ca	Si	Al	Fe	S	K	Mg	Na	P	Ti	Mn	Ba	Sr	Ni	Cu	Rb	Zn	V	Cr	Zr	Pb	Sn	Ce	Mo	As	La	Ga	Y	Co
MS	1.00																													
Ca	-0.77	1.00																												
Si	0.81	-0.99	1.00																											
Al	0.86	-0.97	0.97	1.00																										
Fe	0.91	-0.70	0.74	0.83	1.00																									
S	-0.20	-0.27	0.22	0.18	0.03	1.00																								
K	0.25	-0.78	0.75	0.65	0.20	0.54	1.00																							
Mg	0.33	-0.12	0.10	0.22	0.60	0.18	-0.29	1.00																						
Na	0.48	-0.88	0.86	0.79	0.50	0.60	0.88	0.04	1.00																					
P	0.62	-0.39	0.46	0.46	0.64	-0.08	0.10	0.29	0.20	1.00																				
Ti	0.43	-0.50	0.53	0.41	0.07	-0.27	0.51	-0.62	0.35	0.18	1.00																			
Mn	0.81	-0.50	0.55	0.62	0.74	-0.16	0.05	0.30	0.23	0.75	0.27	1.00																		
Ba	0.49	-0.93	0.90	0.85	0.47	0.50	0.93	-0.02	0.91	0.21	0.43	0.26	1.00																	
Sr	0.33	-0.05	0.09	0.12	0.35	-0.44	-0.18	0.23	-0.11	0.17	-0.03	0.18	-0.15	1.00																
Ni	0.82	-0.77	0.78	0.81	0.70	-0.05	0.47	0.12	0.52	0.54	0.58	0.65	0.62	0.01	1.00															
Cu	0.84	-0.78	0.79	0.88	0.87	0.09	0.40	0.42	0.56	0.56	0.25	0.66	0.63	0.07	0.92	1.00														
Rb	0.32	-0.51	0.47	0.56	0.61	0.48	0.31	0.67	0.54	0.11	-0.46	0.11	0.51	0.17	0.19	0.52	1.00													
Zn	0.93	-0.82	0.83	0.88	0.80	-0.11	0.35	0.28	0.55	0.42	0.45	0.69	0.58	0.18	0.85	0.84	0.37	1.00												
V	0.94	-0.83	0.85	0.89	0.89	-0.04	0.34	0.36	0.59	0.44	0.35	0.66	0.60	0.19	0.79	0.85	0.49	0.95	1.00											
Cr	0.14	-0.05	0.05	0.15	0.51	0.33	-0.19	0.84	0.13	0.21	-0.79	0.13	-0.01	0.23	-0.13	0.24	0.81	0.06	0.23	1.00										
Zr	0.77	-0.77	0.79	0.78	0.74	-0.04	0.49	0.21	0.63	0.22	0.37	0.37	0.60	0.51	0.63	0.66	0.49	0.73	0.80	0.19	1.00									
Pb	0.89	-0.73	0.73	0.82	0.88	-0.06	0.21	0.53	0.49	0.44	0.16	0.68	0.48	0.28	0.73	0.84	0.58	0.95	0.94	0.37	0.73	1.00								
Sn	0.82	-0.79	0.81	0.82	0.67	-0.08	0.51	0.04	0.54	0.52	0.66	0.63	0.64	0.00	0.99	0.88	0.14	0.85	0.79	-0.21	0.63	0.71	1.00							
Ce	0.90	-0.72	0.75	0.74	0.76	-0.22	0.25	0.24	0.50	0.56	0.46	0.69	0.42	0.34	0.69	0.65	0.26	0.89	0.87	0.11	0.72	0.86	0.69	1.00						
Mo	0.65	-0.66	0.68	0.65	0.38	-0.06	0.49	-0.25	0.47	0.32	0.84	0.54	0.56	-0.18	0.83	0.61	-0.20	0.72	0.62	-0.54	0.41	0.47	0.88	0.57	1.00					
As	-0.01	0.16	-0.18	-0.03	0.34	0.20	-0.40	0.83	-0.11	0.01	-0.89	0.01	-0.21	0.24	-0.29	0.10	0.72	-0.06	0.07	0.95	0.03	0.26	-0.37	-0.06	-0.66	1.00				
La	0.16	-0.04	0.06	0.07	0.05	-0.24	-0.12	-0.04	-0.14	0.51	0.22	0.26	-0.04	-0.47	0.35	0.26	-0.26	0.21	0.13	-0.23	-0.34	0.11	0.36	0.19	0.35	-0.25	1.00			
Ga	-0.27	0.37	-0.38	-0.28	0.07	0.10	-0.45	0.62	-0.29	-0.07	-0.91	-0.17	-0.34	0.13	-0.50	-0.15	0.52	-0.36	-0.22	0.83	-0.18	-0.06	-0.57	-0.31	-0.84	0.90	-0.22	1.00		
Y	0.94	-0.74	0.78	0.82	0.79	-0.20	0.30	0.14	0.43	0.66	0.56	0.86	0.51	0.09	0.90	0.84	0.13	0.88	0.86	-0.06	0.61	0.78	0.90	0.80	0.79	-0.22	0.36	-0.41	1.00	
Co	0.22	-0.19	0.16	0.30	0.55	0.39	-0.07	0.84	0.21	0.14	-0.71	0.23	0.16	0.08	0.06	0.43	0.86	0.21	0.33	0.92	0.24	0.49	-0.03	0.10	-0.36	0.89	-0.21	0.74	0.08	1.00

The elements are recalculated from oxides and sorted by greatest values (see original data in Kabanov *et al*., 2012). Elements with greatest values below 10 ppm are excluded.

DOI: 10.1002/gj

Table 5. Pearson *r* correlation matrix of MS and elements in the upper Zaborie Group of Novogurovsky (Units 34–37 in Fig. 6) and Dashkovka (Units 1–8 in Fig. 6)

	MS	Si	Ca	Al	Mg	Fe	K	Na	Ti	S	P	Mn	Ba	Zn	Sr	Pb	Ni	Cr	Rb	Cu	V	Zr	Ce	La	Sn	Y	Co	Nb	Ga	As	Cs
MS	1.00																														
Si	0.67	1.00																													
Ca	-0.65	-0.96	1.00																												
Al	0.57	0.90	-0.83	1.00																											
Mg	0.52	0.72	-0.81	0.73	1.00																										
Fe	0.90	0.83	-0.83	0.72	0.75	1.00																									
K	0.60	0.88	-0.82	0.95	0.63	0.65	1.00																								
Na	0.51	0.77	-0.63	0.87	0.57	0.70	0.74	1.00																							
Ti	0.94	0.81	-0.79	0.73	0.63	0.87	0.79	0.59	1.00																						
S	0.38	0.35	-0.30	0.52	0.50	0.59	0.31	0.70	0.28	1.00																					
P	-0.50	0.21	-0.23	0.37	0.30	-0.15	0.25	0.28	-0.30	0.25	1.00																				
Mn	-0.69	-0.77	0.87	-0.65	-0.70	-0.69	-0.75	-0.28	-0.82	-0.06	0.01	1.00																			
Ba	0.61	0.84	-0.76	0.96	0.61	0.65	0.98	0.77	0.77	0.41	0.23	-0.69	1.00																		
Zn	-0.38	0.33	-0.33	0.49	0.32	-0.13	0.47	0.27	-0.12	0.10	0.93	-0.20	0.44	1.00																	
Sr	-0.76	-0.88	0.88	-0.76	-0.57	-0.75	-0.87	-0.54	-0.91	-0.12	0.04	0.89	-0.80	-0.17	1.00																
Pb	-0.44	0.27	-0.27	0.44	0.28	-0.18	0.40	0.24	-0.19	0.10	0.95	-0.13	0.38	1.00	-0.10	1.00															
Ni	-0.43	0.35	-0.29	0.46	0.24	-0.11	0.37	0.43	-0.19	0.15	0.92	0.03	0.35	0.90	-0.07	0.91	1.00														
Cr	0.83	0.70	-0.71	0.73	0.67	0.89	0.65	0.61	0.76	0.65	-0.10	-0.66	0.70	-0.04	-0.62	-0.10	-0.13	1.00													
Rb	0.58	0.47	-0.47	0.44	0.33	0.47	0.50	0.11	0.55	0.09	-0.23	-0.66	0.56	0.01	-0.49	-0.05	-0.20	0.69	1.00												
Cu	-0.31	0.46	-0.38	0.49	0.26	0.02	0.37	0.51	-0.11	0.16	0.81	0.01	0.35	0.78	-0.12	0.78	0.96	-0.06	-0.14	1.00											
V	0.91	0.87	-0.85	0.78	0.70	0.92	0.79	0.64	0.96	0.41	-0.19	-0.83	0.80	-0.02	-0.89	-0.09	-0.09	0.82	0.63	0.01	1.00										
Zr	0.83	0.81	-0.83	0.68	0.56	0.77	0.76	0.40	0.89	0.06	-0.23	-0.90	0.73	-0.02	-0.88	-0.09	-0.14	0.77	0.76	-0.04	0.87	1.00									
Ce	0.95	0.82	-0.81	0.73	0.60	0.90	0.78	0.58	0.97	0.29	-0.29	-0.83	0.76	-0.13	-0.89	-0.20	-0.20	0.85	0.62	-0.10	0.94	0.94	1.00								
La	0.54	0.69	-0.63	0.78	0.50	0.61	0.75	0.72	0.61	0.27	0.09	-0.46	0.73	0.17	-0.57	0.12	0.22	0.65	0.33	0.28	0.54	0.66	0.71	1.00							
Sn	-0.32	0.47	-0.41	0.56	0.33	0.00	0.47	0.49	-0.07	0.16	0.90	-0.10	0.44	0.91	-0.19	0.91	0.99	-0.04	-0.13	0.96	0.03	-0.01	-0.08	0.30	1.00						
Y	0.42	0.80	-0.84	0.87	0.74	0.60	0.85	0.64	0.59	0.29	0.46	-0.71	0.79	0.55	-0.70	0.50	0.47	0.62	0.34	0.46	0.58	0.68	0.66	0.83	0.57	1.00					
Co	-0.03	0.43	-0.54	0.15	0.41	0.24	0.08	-0.04	0.04	-0.12	0.36	-0.41	0.02	0.33	-0.21	0.32	0.35	0.14	0.26	0.47	0.18	0.31	0.10	0.01	0.40	0.31	1.00				
Nb	0.84	0.84	-0.80	0.76	0.46	0.78	0.85	0.55	0.90	0.23	-0.17	-0.83	0.83	0.04	-0.93	-0.03	-0.06	0.78	0.68	0.01	0.90	0.93	0.94	0.64	0.06	0.65	0.12	1.00			
Ga	0.63	0.07	-0.09	-0.05	0.14	0.45	-0.06	-0.09	0.40	0.09	-0.75	-0.26	0.01	-0.70	-0.10	-0.73	-0.75	0.55	0.64	-0.61	0.41	0.48	0.47	0.15	-0.71	-0.13	0.03	0.32	1.00		
As	-0.48	-0.44	0.36	-0.25	-0.16	-0.48	-0.26	-0.48	-0.54	-0.11	0.28	0.17	-0.20	0.31	0.51	0.33	0.09	-0.08	0.32	-0.03	-0.45	-0.24	-0.43	-0.22	0.03	-0.10	0.12	-0.35	0.07	1.00	
Cs	0.99	0.72	-0.69	0.64	0.55	0.93	0.64	0.60	0.93	0.46	-0.41	-0.68	0.66	-0.31	-0.76	-0.37	-0.34	0.89	0.57	-0.23	0.91	0.83	0.96	0.62	-0.23	0.49	-0.02	0.86	0.59	-0.46	1.00

The elements are recalculated from oxides and sorted by greatest values (original data from Kabanov *et al*., 2012). Elements with greatest values below 10 ppm are excluded.

The siliciclastic association is represented in available samples almost exclusively by shales, which tend to be enriched in the majority of measured elements (Tables 3–5).

6.3. Manganese and trace metals

The overall concentration of Mn shows a moderate increase from the Upper Venev to the basal Gurovo formations and decline in the upper half of the Glazechnya Shale and the Dashkovka Shale (Figs. 4 and 6). In the Ignatova Gora Member (Lower Tarusa Fm.), manganese remains at low background values of 0.02–0.04% and shows a weak depression in the thin shale overlying the Forino Disconformity (Unit 44 of Polotnyanyi Zavod and Unit 27 of Novogurovsky; Kabanov *et al*., 2014). In Novogurovsky this shale is strongly enriched in Cu, Ni, Zn, and Pb. These peaks are most distinct in the Cu–Ni bundle where the enrichment factor for each element (greatest value divided by IQM) attain 5–10 against the background of the underlying and overlying Tarusa rocks. This trace-metal enrichment is also expressed in Al-normalized values (right-end curves in Fig. 6). At the same stratigraphic level in Polotnyanyi Zavod, the enrichment of trace metals is weaker and not expressed on Al-normalized logs (Fig. 4). This enrichment horizon also has a characteristic spike in iron and magnetic susceptibility. Based on these signatures, this shale must be genetically similar to the MEHs of the Oka Group (e.g. Units 15, 18–19, and 29 of Polotnyanyi Zavod and Units 4, 10, and 12 of Novogurovsky).

In the Byokhovo Member (of the upper Tarusa Fm.), trace-metal curves remain featureless, and the spike of Al-normalized curves in Unit 30 of Novogurovsky is only related to a low content of alumina (Fig. 6). The lower Gurovo (Units 32–3d of Novogurovsky) exhibits fluctuating enrichment of Fe, Cu, Ni, Pb, and Zn. Noteworthy, these fluctuations are mostly inverse to fluctuations of Mn, which is especially distinct in Units 34a–34e (Fig. 6). In this interval excluding the basal sample NG-34a-n, Pearson *r* (Mn, Cu) = −0.47, (Mn, Ni) = −0.42, (Mn, Zn) = −0.49, and (Mn, Pb) = −0.43. Manganese here also shows strong negative correlation with V (−0.89), Cr (−0.46), and Co (−0.53). Limestone beds in this interval are Mn-rich and depleted in trace metals and iron, whereas black shales between these limestones show an inverse relation. It is remarkable that normalization to alumina reduces but does not eliminate or inverse these peaks, indicating that enrichment of Units 34a–34d in trace metals is most probably authigenic rather than related to detrital components. A note of caution should be taken with regard to material limitations. Our material from Units 34a–34e of Novogurovsky is limited to seven samples, so that the above-described pattern should be verified with denser sampling and study of mineral carriers of trace metals at the earliest opportunity.

DOI: 10.1002/gj

In the overlying Glazhechnya Shale of the Dashkovka section, the Mn and trace-metal curve mostly stay at low background values (Fig. 6). Manganese and Al-normalized trace metals give concordant spikes in the top limestone (Unit 9, OLM member in Fig. 6) and a less pronounced spike in a limestone bed below (Unit 7 in Fig. 6). Unit 9 is also strongly dolomitized (MgO peak in Fig. 6) and is imprinted by a palygorskitic calcrete of the Dashkovka palaeosol (Kabanov *et al*., 2012). The strongest manganization (0.33% of Mn) is found in a sample from the base of Unit 10—a thin marly bed with 'desert roses' of gypsum. This thin bed may represent the uppermost (topsoil) part of the Dashkovka palaeosol or playa sediment of the early transgressive phase of Protvian time (Kabanov *et al*., 2012).

Kabanov *et al*. (2012) considered two possible interpretations of the Mn spike at the Dashkovka Disconformity. It could be an accumulation in a subaerial environment through multiple redox cycles close to the present-day surface (rock varnish) or in the tissues of xerophytic vegetation, similar to aridisol profiles described from the Middle Pennsylvanian of the same region (Kabanov *et al*., 2010). Alternatively, Mn could precipitate along fluctuating ground water level that followed an impermeable shale top during protracted mid-Carboniferous subaerial exposure. The groundwater interpretation can also accommodate relative enrichment in trace metals in several samples just below and just above the disconformity (Fig. 6).

7. PHOSPHORUS IN OKA AND ZABORIE GROUPS

Phosphorus values stay close to 0% in the Oka Group (figs. 5 and 3 in Alekseev *et al*., in press) and tend to increase in the Zaborie Group (Fig. 6; Kabanov *et al*., 2012; Alekseev *et al*., in press). This distribution is in agreement with the dramatic increase of conodont numbers from the Viséan into the Serpukhovian (from <3 specimens/kg in the Oka Group to >100 specimens/kg in the Zaborie group; Gibshman *et al*., 2009). The argillaceous limestones and shales of the Gurovo Formation are also enriched in fish sclerites in response to progressive deepening and eutrophication of the basin (Kabanov *et al*., 2012, 2014). In the Tarusa and lower Gurovo (Beds 25–34d of Novogurovsky), phosphorus shows direct correlation with shaliness—its content is higher in more argillaceous, deeper-water *Zoophycos* intervals (averaging 0.26% P_2O_5) than in shallower-water limestones (averaging 0.09% P_2O_5). The upper part of the Glazechnya Shale (Units 34e–36) is somewhat depleted in biogenic phosphate (0.04–0.1% P_2O_5). As long as no reliable evidence of seafloor or diagenetic phosphatization processes exists, all phosphorus in our samples appears to be biogenic skeletal in origin.

8. DISCUSSION

8.1. Siliciclastic provenance

The Oka siliciclastic units of Polotnyanyi Zavod are notably rich in Fe, Ti, and Zr (Fig. 4). The non-truncated average concentration of Ti in three siliciclastic units MH_{T1}, MH_{T2}, and VN_{T1} is 0.65% (IQM 0.60%) and peaks at 1.6%. The average concentration of Fe is 5.9% (IQM 3.2%) with the highest value of 31.7% (Alekseev *et al*., in press). In this sedimentary system, the average concentrations of Ti and Fe are double compared to the Clarke values of Ti estimated for the upper continental crust (0.31% for Ti and 3.09% for Fe; Ronov and Yaroshevskiy, 1968; Wedepohl, 1995). Enrichment in Zr is even higher (0.07% in siliciclastic units of Polotnyanyi Zavod against the 0.024% Clarke value of Wedepohl, 1995). These values show residual enrichment left after farfield depletion of fluvial sands in ore minerals, as both proposed crystalline sourcelands are located several hundreds of kilometre away from Polotnyanyi Zavod. These enrichments are consistent with Lower Proterozoic Ti-rich Fe–quartzites (BIF type) and Devonian volcanic fields of the central and northern Voronezh High. This region hosts one of the world's largest iron ore resources in mafic structural blocks (Bekker *et al*., 2010; Dagelaysky, 1997; Gusel'nikov, 1981; Shchipansky and Bogdanova, 1996). Nearfield placers of Ti-rich magnetite and ilmenite are known from the Upper Devonian, Cretaceous, and Cenozoic (Savko *et al*., 2012; Shevyrev *et al*., 2004). The richest placer with 51.8% of ilmenite ($FeTiO_3$) in the heavy grain fraction is reported from the upper Frasnian of the north-central Voronezh High (Savko *et al*., 2012). In contrast, the predominantly felsic basement of the Belorussian High is generally poor in iron and associated metals (Pap, 1971). The Fennoscandian Shield is also predominantly felsic (Lahtinen, 2012; Lauri *et al*., 2012), and of the three possible provinces, it is the most remote from the studied sections (Fig. 2).

The Oka shales and siltstones rich in Fe, Ti, and trace metals were deposited in environments ranging from fluvial-overbank deposits to slowly accumulating, low-pH coastal marshlands and their extensions into shallow sea (Alekseev *et al*., in press; Kabanov *et al*., 2014). In such environments, iron precipitated as siderite nodules (now mostly weathered into limonite) and probably some pyrite. These metal enrichment horizons (MEHs) are distinct by vigorous *Stigmaria* development indicating dense vegetation composed of lycopsid (mangrove-like or mangal ecotype; Alekseev *et al*., in press; Kabanov *et al*., 2014).

The Steshevian-time black-shale basin (Gurovo Formation), previously interpreted as lagoonal, based on its spatially localized shape (Fig. 3B; Osipova and Belskaya, 1965; Belskaya *et al*., 1975; Makhlina *et al*., 1993), appears to be a relatively deep-water facies, very much different from the

DOI: 10.1002/gj

Oka shales (Kabanov *et al*., 2012). The non-truncated average of Ti for the Glazechnya and Dashkovka shale members is 0.22% (IQM 0.23%), and that of Fe is 3.2% (IQM 3.1%), which is at the Clarke level (Wedepohl, 1995). Concentrations of Fe and Ti are relatively steady in samples (low standard deviations of 0.13 and 2.1, respectively; Table 1). Zirconium shows depletion (0.0066% mean and 0.0065% IQM against 0.0237% Clarke value). Since configuration of the Gurovo shale basin favours its development in front of a southerly or southwesterly located delta (Kabanov *et al*., 2012), the Voronezh sourceland here seems to be most likely. With the present-day knowledge, differences in bulk geochemical signatures can be ascribed to offshore depletion (sink of heavy elements in delta-plain marshes) and/or greater contribution from felsic crystalline blocks of the Voronezh Land; however, other possible controls such as differential dissolution of mineral carriers of heavy metals should not be discounted.

8.2. *Origin of trace-metal enrichments in the Oka Group*

The MEH-hosting coaly ('sooty') shales present on disconformities and in lower parts of siliciclastic units of the Oka Group are interpreted as slowly accumulated deposits of low-pH marshes in a sluggish fluvial system (everglades-type) resulted from a regime of transgressive ponding (Alekseev *et al*., in press; Kabanov *et al*., 2014). The shale at the top of the Forino Disconformity within the Tarusa Formation (Fig. 1) also belongs to the MEH type. Geochemical signatures of MEHs with notable enrichment in Cu, Ni, Pb, Zn, Cr, and Co probably reflect authigenic enhancement of these elements. If trace metals are bound in ferric nodules, their enhancement may be explained by fluvial supply in dissolved form and precipitation as sulphides in the anoxic underpeat environment. However, heavy metals also can be bound in clays. Mn-rich levels in the base of the siliciclastic bed MH_{T1} of Polotnyanyi Zavod and of Novogurovsky indicate accumulation at the redox barrier. In other parts of the Oka section, featureless curves of Mn and trace elements are in agreement with lithofacies observations that suggest the absolute prevalence of extremely shallow-water and sufficiently oxygenated sedimentary environments (Kabanov *et al*., 2014).

8.3. *Bottom oxygenation regime of Gurovo shale basin*

The above-described pattern of Mn, Cu, Ni, Pb, and Zn in the lower Glazechnya Shale (Units 34a–34d of Novogurovsky; Fig. 6) have been interpreted as a signature of seafloor oxygen deficiency (Kabanov *et al*., 2012). By the oxygen content, sedimentary environments are usually classified into oxic (>2.0 ml/l O_2), hypoxic or isoxic (~0.2–2.0 ml/l O_2), anoxic non-sulphidic (<0.2 ml/l O_2 and 0 ml/l H_2S), and anoxic sulphidic or euxinic (0 ml/l O_2, and >0 ml/l H_2S; Calvert and Pedersen, 1993). The Mn-rich samples collected from carbonate-rich beds record oxygen-poor (about 0.2 ml/l O_2) environments when the redox barrier levelled with the sediment surface, whereas Mn-poor and sulphidophile-rich shaly intervals record transitions to anoxic settings. The overall weak expression of these element fluctuations may be caused by the sampling method with averaging of at least 10 cm-thick intervals. Lack of significant peaks in Al-normalized values (Pb/Al, Cu/Al, Ni/Al, and Zn/Al) indicates that persistent bottom anoxia did not develop. The relatively weak pumping of trace metals and gradual decline of Mn fluctuations in shales above the Unit 34d suggest progressive increase in bottom oxygenation in the later stages of 'Steshevian basin' development. The notable vanadium enrichment in the Glazechnya Shale is difficult to interpret. The trace-fossil signatures with *Zoophycos* and *Chondrites* tiers and accumulation of silicisponge spicules found in the base of this unit are consistent with hypoxic, and probably intermittently anoxic, environment established below the pycnocline (Kabanov *et al*., 2012).

9. CONCLUSIONS

Reconnaissance bulk geochemical logs made for three outcrop sections stratigraphically cover the Oka and Zaborie groups of the upper Viséan–lower Serpukhovian interval in the type area for the Serpukhovian Stage in the Moscow Basin. In this paper, previously published data (Alekseev *et al*., in press; Kabanov *et al*., 2012) are supplemented by new data from the Oka Group of the Novogurovsky section, and geochemical data from Polotnyanyi Zavod are published in full for the first time.

Geochemical analysis of the Oka Group is based on 173 samples from Polotnyanyi Zavod and Novogurovsky. The first section contains thick (over 1 m) siliciclastic units that wedge out eastward to thin (5–15 cm) coal-capped shales in the second section (Fig. 1). Corresponding to this off-sourceland gradient, siliciclastics in Novogurovsky are 2 to 2.5 times more depleted in Fe, Ti, and Zr compared to Polotnyanyi Zavod. Bulk iron in the studied sections shows the strongest correlation with magnetic susceptibility. Initially introduced into the sedimentary system by terrigenous influx, Fe was redistributed into ferruginized horizons in ponded conditions of coastal low-pH marshlands (Alekseev *et al*., in press). Noteworthy, almost all iron-rich shales coincide with dense *Stigmaria* penetrations and are enriched in Cu, Ni, Pb, Zn, and other trace elements. The thin shale at the Forino Disconformity in the lowermost Zaborie Group belongs in the same type of metal enrichment horizons (MEHs). However, well-drained environments of

DOI: 10.1002/gj

palaeokarst formation and alkaline everglades (Akulshino palustrine event), also riddled with *Stigmaria*, did not accumulate iron and trace metals.

The thin shale seam (Unit 38) found close to the Viséan–Serpukhovian boundary in Polotnyanyi Zavod has unusually high values of high Rb (0.2%) and Sr (0.45%). Rubidium is generally alien to the studied sedimentary system (close to 0 in other samples), and Sr occurs in trace quantities (0.02–0.05%) predominantly in limestones. Based on these Rb and Sr signatures, the shale of Unit 38 is likely to contain a volcanigenic component from a distal source, making it prospective for high-precision dating of the stage boundary.

The Zaborie Group is assessed by 23 samples from Polotnyanyi Zavod, 25 samples from Novogurovsky, and 12 samples from Dashkovka. The shales of the Gurovo Formation are moderately enriched in Fe and Ti. The upper part of the Glazechnya Shale has a δMS exceeding 0, which may indicate a ferrimagnetic form of iron (however, new tests for iron mineral forms are required to confirm this). In the transition from the Glazechnya montmorillonitic shales to the Dashkovka palygorskitic shales (XRD data from Kabanov *et al*., 2012), MgO shifts from 1.3% of interquartile mean (IQM) to 7.3% IQM, which is interpreted as a signature of progressive shoaling of the Gurovo shale basin and increased evaporative pumping of Mg (climatic aridization).

Phosphorus values remain close to 0% in the Oka Group and tend to increase in the Zaborie Group, in agreement with dramatic increase of conodont numbers from the Viséan into the Serpukhovian in response to a marine transgression. Phosphorus also shows strong correlation with the shaliness of marine sediments, which is especially distinct in the lower Zaborie carbonate-dominated section. As long as no reliable evidence of seafloor or diagenetic phosphatization processes exists, all phosphorus in our samples appears to be biogenic skeletal in origin.

The concentration of Mn shows an overall moderate increase from the Upper Venev to the basal Gurovo formations and declines in the upper half of the Glazechnya Shale and the Dashkovka Shale. The lower 4.0 m of the Glazechnya Member at Novogurovsky exhibits fluctuating enrichment in Fe, Cu, Ni, Pb, Zn, V, Cr, and Co. These fluctuations are mostly inverse to fluctuations of Mn. Thin limestone beds in this interval are Mn-rich and depleted in trace metals and iron, whereas black shales between limestones show an inverse relation. Normalization to alumina reduces but does not eliminate these peaks. This pattern has been interpreted as a signature of seafloor oxygen deficiency (Kabanov *et al*., 2012). The Mn-rich samples record oxygen-poor (about 0.2 ml/l O_2) environments when redox barrier levelled with the sediment surface, whereas Mn-poor black shales enriched in Fe and trace metals record transitions to anoxic settings. This interval probably represents the maximum flooding event of the lower Serpukhovian transgression.

The enrichment of Oka siliciclastic units of Polotnyanyi Zavod in Fe, Ti, and Zr that are two to three times higher than Clarke values indicate their provenance from the ore-rich Voronezh Land. The westerly flux previously regarded as an option in palaeogeographic reconstructions is discarded for the studied sections. The Gurovo Shale shows Fe and Ti at Clarke values and depletion in Zr. However, configuration of this shale basin strongly favours Voronezh Land as the siliciclastic provenance. Differences in bulk geochemical signatures between Oka and Steshevian shales can be ascribed to offshore depletion in ore elements and/or greater contribution from the felsic crystalline blocks of the Voronezh Land.

ACKNOWLEDGEMENTS

This work was supported by the Russian Foundation for Basic Research, grant 12-04-00387, the Programme of Presidium RAS N28 'Biosphere Origin and Evolution', and the 'Program of Competitive Growth of Kazan Federal University among World`s Leading Academic Centres' of the Russian Government. Critical reviews by Ondrej Bábek (Masaryk University of Brno) and Keith Dewing (GSC, Natural Resources Canada) and thorough editorial work by Ian D. Somerville (University College, Dublin) led to very significant improvements of the manuscript. The authors are thankful to Olga Orlova (Lomonosov Moscow State University) and Aleksei Mazaev (Paleontological Institute RAS) for assistance with field works and sampling. Aleksandr S. Alekseev (Moscow State University) and Svetlana V. Bogdanova (Lund University) are cordially thanked for help with regional geological data. The first author has worked on this manuscript at Geological Survey of Canada (Earth Science Sector of Natural Resources Canada, contribution number 20140215).

REFERENCES

Akimets, V.S., **Golubtsov, V.K.**, **Voznyachuk, L.N.**, **Kichkina, M.S.**, **Manykin, S.S.**, **Makhnach, A.S.**, **Mityanina, I.V.**, **Puzanov, L.T. 1971**. History of geological development. In: *Geologiya SSSR*. Tom III. *Belorusskaya SSR*, Leonovich, P.A. (ed.). Nedra: Moscow; 366–432. (In Russian)

Alekseev, A.O., **Kabanov, P.B.**, **Alekseeva, T.V.**, **Kalinin, P.E.** In press. Iron, magnetic susceptibility, and XRF characterization of an upper Mississippian cyclothemic section Polotnyanyi Zavod (Moscow Basin, Russia). In: *Magnetic Susceptibility Application—A Window onto Ancient Environments and Climatic Variations*, da Silva, A.C., Whalen, M.T., Hladil, J., Chadimova, L., Chen, D., Spassov, S., Boulvain, F., Devleeschouwer, X. (eds). Geological Society: London, Special Publication.

Alekseeva, T., **Kabanov, P.**, **Alekseev, A. 2012**. Palustrine beds in late Mississippian epeiric-sea carbonate succession (southern Moscow Basin, Russia) as calcimagnesian pedosedimentary systems. In: *Sixth Mid-European Clay Conference Book of Abstracts*. Pruhonice: Czech Republic; 29. http://www.mecc2012.org/doc/informator49_6MECC_BookofAbstracts_www.pdf

DOI: 10.1002/gj

Algeo, T.J., **Maynard, J.B. 2004**. Trace-element behavior and redox facies in core shales of Upper Pennsylvanian Kansas-type cyclothems. *Chemical Geology* **206**, 289–318.

Bekker, A., **Slack, J.F.**, **Planavsky, N.**, **Krapež, B.**, **Hofmann, A.**, **Konhauser, K.O.**, **Rouxel, O.J. 2010**. Iron formation: the sedimentary product of a complex interplay among mantle, tectonic, oceanic, and biospheric processes. *Economic Geology* **105**, 467–508.

Belskaya, T.N., **Ivanova, E.A.**, **Ilkhovskii, R.A.**, **Maslennikov, V.P.**, **Makhlina, M.K.**, **Mikhailova, E.V.**, **Osipova, A.I.**, **Reitlinger, E.A.**, **Shik, E.M.**, **Shik, S.M.**, **Yablokov, V.S. 1975**. *Field Excursion Guidebook for the Carboniferous Sections of the Moscow Basin*. Nauka: Moscow; 176. (Bilingual)

Birina, L.M., **Sorskaya, L.S.**, **Rozhdenstvenskaya, K.K.**, **Fomina, E.V. 1971**. Carboniferous system. Lower series. In: *Geologiya SSSR. Vol. IV. Tsentr Evropeiskoi chasti SSSR. Pt.1: Geologicheskoe opisanie*, Leonenko, I.N., Shik, S.M. (eds). Nedra: Moscow; 194–258. (in Russian)

Calvert, S.E., **Pedersen, T.F. 1993**. Geochemistry of recent oxic and anoxic marine sediments: implications for the geological record. *Marine Geology* **113**, 67–88.

Dagelaysky, V.B. 1997. Chapter 6. The Voronezh crystalline massif. In: *Precambrian ore deposits of the East European and Siberian Cratons*, Rundqvist, D.V., Gillen, C. (eds). Developments in Economic Geology, **30**, 155–172.

Ellwood, B.B., **Tomkin, J.H.**, **El Hassani, A. P.**, **Bultync, C.E.**, **Brett, C.E.**, **Schindler, R.F.**, **Bartholomew, A.J. 2011**. A climate-driven model and development of a floating point time scale for the entire Middle Devonian Givetian Stage: a test using magnetostratigraphy susceptibility as a climate proxy. *Palaeogeography, Palaeoclimatology, Palaeoecology* **304**, 85–95.

Gibshman, N.B., **Kabanov, P.B.**, **Alekseev, A.S.**, **Goreva, N.V.**, **Moshkina, M.A. 2009**. Novogurovsky quarry. Upper Viséan and Serpukhovian. In: *Type and Reference Carboniferous Sections in the South Part of the Moscow Basin*, Alekseev, A.S., Goreva, N.V. (eds). Field Trip Guidebook of International I.U.S.C. Field Meeting, Paleontological Institute RAS: Moscow, 13–44.

Gusel'nikov, V.N. 1981. Iron–ore associations and volcanism of the Kursk magnetic anomaly (KMA). *International Geology Review* **23**, 571–580.

Harris, N.B., **Mnich, C.A.**, **Selby, D.**, **Korn, D. 2013**. Minor and trace element and Re–Os chemistry of the Upper Devonian Woodford Shale, Permian Basin, west Texas: Insights into metal abundance and basin processes. *Chemical Geology* **356**, 76–93.

Hölttä, P., **Balagansky, V.**, **Garde, A.A.**, **Mertanen, S.**, **Peltonen, P.**, **Slabunov, A.**, **Sorjonen-Ward, P.**, **Whitehouse, M. 2008**. Archean of Greenland and Fennoscandia. *Episodes* **31**, 13–19.

Kabanov, P., **Alekseeva, T.**, **Alekseev, A.**, **Alekseeva V.**, **Gubin, S. 2010**. Paleosols in Late Moscovian (Carboniferous) marine carbonates of East European Craton revealing "Great Calcimagnesian Plain" paleolandscapes. *Journal of Sedimentary Research* **80**, 195–215.

Kabanov, P.B., **Alekseeva, T.V.**, **Alekseev, A.O. 2012**. Serpukhovian Stage of the Carboniferous in its type area: facies, geochemistry, mineralogy, and section correlation. *Stratigraphy and Geological Correlation* **20**(1), 15–41.

Kabanov, P.B., **Alekseev, A.S.**, **Gabdullin, R.R.**, **Gibshman, N.B.**, **Bershov, A.**, **Naumov, S.**, **Samarin, E. 2013**. Progress in sequence stratigraphy of upper Visean and lower Serpukhovian of southern Moscow Basin, Russia. *Newsletter on Carboniferous Stratigraphy* **30**, 55–65.

Kabanov, P.B., **Alekseev, A.S.**, **Gibshman, N.B.**, **Gabdullin, R.R.**, **Bershov, A.V. 2014**. The upper Viséan–Serpukhovian in the type area for Serpukhovian Stage (Moscow Basin, Russia). Part 1. Sequences, disconformities, and biostratigraphic summary. *Geological Journal*. DOI: 10.1002/gj.2612

Lahtinen, R. 2012. Main geological features of Fennoscandia. *Geological Survey of Finland Special Paper* **53**, 13–18.

Lauri, L.S., **Mikkola, P.**, **Karinen, T. 2012**. Early Paleoproterozoic felsic and mafic magmatism in the Karelian province of the Fennoscandian shield. *Lithos* **151**, 74–82.

Makhlina, M.K., **Vdovenko, M.V.**, **Alekseev, A.S.**, **Byvsheva, T.V.**, **Donakova, L.M.**, **Zhulitova, V.E.**, **Kononova, L.I.**, **Umnova, N.I.**, **Shik, E.M. 1993**. *Nizhniy karbon Moskovskoy sineklizy i Voronezhskoy anteklizy*. Moscow: Nauka (In Russian).

Nikishin, A.M., **Ziegler, P.A.**, **Stephenson, R.A.**, **Cloetingh, S.A.P.L.**, **Furne, A.V.**, **Fokin, P.A.**, **Ershov, A.V.**, **Bolotov, S.N.**, **Korotaev, M. V.**, **Alekseev, A.S.**, **Gorbachev, V.I.**, **Shipilov, E.V.**, **Lankreijer, A.**, **Bembinova, E.Y.**, **Shalimov, I.V. 1996**. Late Precambrian to Triassic history of the East European Craton: dynamics of sedimentary basin evolution. *Tectonophysics* **268**, 23–63.

Novik, E.O., **Brazhnikova, N.E. 1949**. Carboniferous System. In: *Geologiya SSSR. Tom VI. Bryanskaya, Orlovskaya, Kurskaya, Voronezhskaya I Tamboskaya oblasti. Chast 1. Geologicheskloe opisanie*, Dubyanskiy, A. A., Khakman, S.A. (eds). Gosudarstvennoe Izdatel'stvo Geologicheskoi Literatury: Moscow, 103–135. (In Russian)

Osipova, A.I., **Belskaya, T.N. 1965**. On facies and palaeogeography of Serpukhovian time in Moscow Basin, *Litologiya i poleznye iskopaemye* **1965/5**, 3–17. (in Russian)

Osipova, A.I., **Belskaya, T.N. 1966**. Lithological–paleogeographical maps of the Moscow Syneclise. Sheets 48-51. Aleksin, Mikhailov, Venev, Tarussa, Steshevo, and Protva Times. In: *Altas of the lithological–paleogeographical maps of the USSR. Volume II. Devonian, Carboniferous, and Permian*, Nalivkin, V.D., Posner, V.M. (eds). Ministry of Geology: Leningrad; 1969.

Pap, A.M. 1971. Chapter 4. Stratigraphy. Archean, Lower and Middle Proterozoic (crystalline basement). In: *Geologiya SSSR. Tom III. Belorusskaya SSR*, Leonovich, P.A. (ed.). Nedra: Moscow; 35–51. (In Russian)

Ronov, A. B., **Yaroshevskiy, A. A. 1968**. Chemical structure of the Earth's crust. *Geochemistry International* **5**, 1041–1066.

Savko, A.D., **Zvonarev, A.E.**, **Ivanov, D.A. 2012**. Zirconium–titanium placers of the Voronezh Anteclise: types, epochs and factors of formation, and forecast, *Geology of Ore Deposits* **54**(1), 60–80.

Shatsky, N.S., **Mushenko, A.I. 1949**. Tectonics. In: *Geologiya SSSR. Tom VI. Bryanskaya, Orlovskaya, Kurskaya, Voronezhskaya I Tamboskaya oblasti. Chast 1. Geologicheskloe opisanie*, Dubyanskiy, A.A., Khakman, S. A. (eds). 285–297. Gosudarstvennoe Izdatel'stvo Geologicheskoi Literatury: Moscow, (In Russian)

Shchipansky, A.A., **Bogdanova, S.V. 1996**. The Sarmatian crustal segment; Precambrian correlation between the Voronezh Massif and the Ukrainian Shield across the Dnieper–Donets Aulacogen. *Tectonophysics* **268**, 23–63.

Shevyrev, L.T., **Savko, A.D.**, **Shishlov A.V. 2004**. Evoluziya tektonicheskoi structury Voronezskoi anteklizi i ee endogennii rudogenez. *Trudy Voronezskogo Gosudarstvennogo Universiteta* **25**, 1–192. (in Russian)

Shvetsov, M.S. 1938. History of Moscow Carboniferous Basin during the Dinantian Epoch, *Moskovskiy geologorazvedochnyi institut*. *Trudy* **12**, 3–107. (in Russian)

Tikhiy, V.N. 1941. Stratigraphy and facies of the Carboniferous of northwestern margins of Dnieper–Donets Basin. In: *Bolshoi Donbass*, Gosgeolizdat: Leningrad, Moscow; 130–163. (In Russian)

Wedepohl, K.H. 1995. The composition of the continental crust. *Geochimica et Cosmochimica Acta* **59**, 1217–1232.

SUPPORTING INFORMATION

Additional supporting information may be found in the online version of this article at the publisher's web-site.

APPENDIX 1: XRF geochemical data for Polotnyanyi Zavod (Oka and lower Zaborie Group)

APPENDIX 2: XRF geochemical data for Novogurovsky (Oka Group)